Table 2 Common ADRs occurring in two or more patients

AE (MedDRA term)[a]	Gefitinib 250 mg/day (n=18)	Placebo (n=20)
Abnormal hepatic function	4	0
Acne	2	0
Anorexia	5	1
Cough	2[b]	1
Diarrhea	9	2
Dry skin	3	0
Eczema	8	2
Elevated ALT/AST	2	0
Fatigue	2	0
Gastritis	3[b]	0
Loose stools	4	0
Nausea	3	0
Rash	5	3
Sputum	0	2
Stomatitis	2	0

[a]A patient could have more than one AE.
[b]All were associated with post-operative complications.

Table 3 Grade 3/4 ADRs

AE (MedDRA term)	Grade	Gefitinib 250 mg/day (n=18)	Placebo (n=20)
Abnormal hepatic function	3	1	0
Eczema	3	1	0
Elevated ALT	3	1	0
Neutropenia	3	0	1
Pneumonitis	4	1	0

Table 4 Exposure of patients to gefitinib

	Gefitinib 250 mg/day (n=18)	Placebo (n=20)
Median duration of treatment [days (range)]	86.5 (4–195)	144.0 (20–197)
Dosing period (n)		
<60 days	6	2
60–120 days	9	4
≥ 120 days	3	14
No. dose interruptions (n)		
1	5	6
2	2	2
≥ 3	2	2

Table 5 ADRs leading to patient withdrawals

Adverse event (MedDRA term)	Grade	Gefitinib 250 mg/day (n=18)	Placebo (n=20)
Eczema	2	1	0
Elevated ALT/AST	2	1	0
	3	1	0
Hepatic function abnormalities	2	1	0
	3	1	0
ILD	1	0	1
Impetigo	2	1	0
Neutropenia	3	0	1
Paronychia	2	1	0
Pneumonitis	4	1	0
Pulmonary fibrosis	1	0	1

and one patient experienced grade 4 ILD-type events (pneumonitis) 107 days after starting gefitinib and was withdrawn from the study. The patient with pneumonitis had taken concomitant shosaikoto, a Chinese herbal medicine, and loxoprofen, both of which have previously been shown to induce pneumonitis [15,16]. Twenty-one days later bacterial pneumonia related to methylprednisolone therapy was diagnosed, and the patient subsequently died 37 days later due to both pneumonitis and bacterial pneumonia. In the placebo arm, one patient who experienced cough and grade 1 pulmonary fibrosis had had interstitial changes on their chest X-ray at enrollment, and in a second patient, pre-existing non-specific interstitial pneumonia was exacerbated resulting in grade 1 ILD. In both patients, these conditions persisted following withdrawal of study drug.

Interruptions and withdrawals due to ADRs

ADRs requiring interruptions in therapy were similar between patients receiving gefitinib or placebo (Table 4) and were usually for less than 14 days, although four patients in the gefitinib arm required treatment to be interrupted for 14 days (including one patient whose treatment was interrupted for 20 days). The majority of ADRs leading to withdrawal were usually mild-to-moderate grade 1/2 in severity (Table 5). Grade 3 ADRs leading to withdrawal occurred in two patients receiving gefitinib (hepatic function abnormalities, elevated ALT) and in one patient receiving placebo (neutropenia), and grade 4 pneumonitis led to the withdrawal of one patient who was receiving gefitinib. Following withdrawal of gefitinib treatment, grade 3 abnormal hepatic function and elevated ALT resolved, and grade 3 neutropenia persisted.

AEs associated with post-operative complications

As there are no safety data regarding the use of gefitinib in the post-operative setting, AEs associated with the healing process were examined to provide preliminary safety data on the start of the dosing timing in the adjuvant setting for gefitinib. AEs related to post-operative complications were observed in six patients in the gefitinib arm and four patients in the placebo arm. In the gefitinib arm, the most frequent AEs were grade 1/2 cough (four patients) and gastritis (three patients), and in the placebo arm grade 1/2 pain (three patients). Grade 1 cough, grade 1 supraventricular arrhythmia and grade 2 dyspnea were also experienced by three out of four patients receiving placebo.

Discussion

This trial was designed to compare survival rates in patients with completely resected stage IB–IIIA NSCLC who had received adjuvant therapy with gefitinib 250 mg/day or placebo. However, incidences of ADRs of ILD-

type events in the advanced disease setting have been increasingly reported since gefitinib was launched in Japan, and new recruitment was put on hold on 23 October 2002 at the request of the Ministry of Health, Labor and Welfare. In order to evaluate the ILD and ensure the safety of the trial patients, two separate Co-ordination Committee and IDMC meetings (December 2002 and January 2003) were conducted to discuss the feasibility of continuing the study and management of the trial patients. Based on the updated information on ADRs of interstitial pneumonia, the committees concluded that the study could be continued because the possibility of risk did not exceed that of benefit to enrolled patients. The IDMC also suggested that top priority should be given to assure the safety of the patients receiving gefitinib, and that discontinuation should be considered if flu-like symptoms including difficulty in breathing, fever and coughing occurred.

A 'Supplemental Explanation Sheet and Informed Consent Form' was provided four times to enrolled patients, offered updated information and methods to assure and manage any safety issues, and confirmed the patients' willingness to continue participating in the study. In December 2002, AstraZeneca KK gave the principal investigators the option to suspend gefitinib treatment at once. With the extensive monitoring of the trial patients in terms of safety, there were still an increasing number of withdrawals. In addition, enrollment could not be resumed until the prospective investigation on gefitinib-related ILD was completed. Based on these facts, the sponsor finally decided to terminate the trial in March 2003.

The types of AEs reported in this trial were similar to that already reported in the large phase II IDEAL 1 and 2 trials for patients with locally advanced or metastatic NSCLC [10,11]. Three patients experienced ILD-type events – two in the placebo arm and one patient in the gefitinib arm (this patient was also taking two other medications known to induce ILD) [15,17]. It has generally been observed that a higher frequency of ILD-type events are reported in Japanese patients taking gefitinib compared with those in other south-east Asian countries and the rest of the world (1.6, 0.3, and 0.3%, respectively) [18]. The occurrence of ILD in Japanese patients and the reasons for such an ethnic stratification in ILD incidence following gefitinib treatment require further clarification.

The most common reason for withdrawal in both treatment arms was due to toxicity, with the majority of drug-related AEs being grade 1/2 in severity. In the advanced or metastatic disease setting, few patients who experience grade 1/2 drug-related AEs withdraw from treatment with gefitinib, and in IDEAL 1, which recruited Japanese patients, two out of 103 patients who received gefitinib 250 mg/day withdrew from therapy due to ADRs [18]. Several factors may explain the high number of withdrawals (including withdrawal of treatment for less severe ADRs) reported in this trial data compared with previously reported studies. These reasons include the fact that patients with early-stage NSCLC may be less tolerant of AEs compared with patients with advanced NSCLC who have received prior chemotherapy. In contrast to the other studies, the impact of heavy media coverage surrounding gefitinib-related ILD cannot be ignored.

It has been suggested that the dosage and schedule of gefitinib used in this study may not best suit patients with completely resected NSCLC in terms of tolerability and a number of adjustments may need to be taken into consideration when planning an adjuvant study of gefitinib in the future. It is unlikely that the time frame of 4–6 weeks is too short before starting adjuvant treatment, as other adjuvant trials conducted in Japanese patients have used similar time frames [3,4]. It may be possible to lengthen the duration by which gefitinib could be interrupted for toxicity, since 14 days may be too short for patients recovering from AEs such as hepatic enzyme elevation, or to reduce the dose following toxicity to perhaps 250 mg every other day, although this would require further study into the efficacy of such an approach.

With no experience of using gefitinib in post-operative patients there was a concern that EGFR-TKIs might impact on surgery-related complications (especially on the healing process) due to their mode of action. In order to assess this, the trial was designed to allow a safety review of the first 60 patients. Due to the early termination of the study, we have only 38 patients' (18 on gefitinib) data for review; however, there does not seem to be any impact on surgery-related complications when gefitinib was administered within 4–6 weeks after surgery, as evidenced by a similar number of these AEs that occurred in both groups. This indicates that it may be feasible to administer gefitinib in the adjuvant setting within this time frame.

In conclusion, this is the first study to investigate the use of EGFR-TKIs as adjuvant therapy. Despite the absence of survival data, there were no unexpected AEs seen in the adjuvant setting compared with those already reported for patients with locally advanced or metastatic NSCLC. However, it was observed that there were more AEs leading to withdrawal in the gefitinib arm, even though the majority of AEs were grade 1/2 in severity, suggesting that a daily dose of gefitinib 250 mg may not best suit patients with completely resected NSCLC in terms of tolerability.

Acknowledgements

The following individuals are the principle investigators and IDMC members: Tetsuya Mitsudomi, Aichi Cancer Center, Nagoya; Motoi Aoe, Okayama University School of Medicine, Okayama; Hideyuki Saeki, National Shikoku Cancer Center, Ehime; Katsuhiro Nakagawa, Osaka Prefectural Habikino Hospital, Osaka; Teruaki Koike, Niigata Cancer Center Hospital, Niigata; Chiaki Endo, Tohoku University School of Medicine, Sendai; Makoto Oda, Kanazawa University School of Medicine, Kanazawa; Kohei Yokoi, Tochigi Cancer Center, Tochigi; Toshihiko Iizasa, Chiba University School of Medicine, Chiba; Fumihiro Tanaka, Kyoto University Faculty of Medicine, Kyoto; Akihide Matsumura, National Kinki Chuo Hospital, Osaka; Ichiro Yoshino, Kyusyu University School of Medicine, Fukuoka; Nagahiro Saijo, National Cancer Center, Tokyo; Haruhiko Fukuda, National Cancer Center, Tokyo; Naoki Ishizuka, National Cancer Center, Tokyo; Tomoyuki Goya, Kyorin University Hospital, Tokyo; Ryuzo Ueda, Nagoya University School of Medicine, Nagoya. We thank Dr Carolyn Gray, from Complete Medical Communications, who provided medical writing support on behalf of AstraZeneca. Iressa is a trademark of the AstraZeneca group of companies

References

1 Ries LAG, Eisner MP, Kosary CL, Hankey BF, Miller BA, Clegg L, *et al. SEER cancer statistics review*; 2004. http://seer.cancer.gov/csr/1975_2001/.

2 Martini N, Bains MS, Burt ME, Zakowski MF, McCormack P, Rusch VW, *et al.* Incidence of local recurrence and second primary tumors in resected stage I lung cancer. *J Thorac Cardiovasc Surg* 1995; **109**:120–129.

3 Kato H, Ichinose Y, Ohta M, Hata E, Tsubota N, Tada H, *et al.* A randomized trial of adjuvant chemotherapy with uracil–tegafur for adenocarcinoma of the lung. *N Engl J Med* 2004; **350**:1713–1721.

4 Wada H, Hitomi S, Teramatsu T. Adjuvant chemotherapy after complete resection in non-small-cell lung cancer. West Japan Study Group for Lung Cancer Surgery. *J Clin Oncol* 1996; **14**:1048–1054.

5 Non-Small Cell Lung Cancer Collaborative Group. Chemotherapy in non-small cell lung cancer: a meta-analysis using updated data on individual patients from 52 randomised clinical trials. *Br Med J* 1995; **311**:899–909.

6 Tanaka F, Miyahara R, Ohtake Y, Yanagihara K, Fukuse T, Hitomi S, *et al.* Advantage of post-operative oral administration of UFT (tegafur and uracil) for completely resected p-stage I–IIIa non-small cell lung cancer (NSCLC). *Eur J Cardiothorac Surg* 1998; **14**:256–262.

7 Arriagada R, Bergman B, Dunant A, Le Chevalier T, Pignon JP, Vansteenkiste J. Cisplatin-based adjuvant chemotherapy in patients with completely resected non-small-cell lung cancer. *N Engl J Med* 2004; **350**:351–360.

8 Endo C, Saito Y, Iwanami H, Tsushima T, Imai T, Kawamura M, *et al.* A randomized trial of postoperative UFT therapy in p stage I, II non-small cell lung cancer: North-east Japan Study Group for Lung Cancer Surgery. *Lung Cancer* 2003; **40**:181–186.

9 Wada H, Miyahara R, Tanaka F, Hitomi S. Postoperative adjuvant chemotherapy with PVM (Cisplatin + Vindesine + Mitomycin C) and UFT (Uracil + Tegafur) in resected stage I–II NSCLC (non-small cell lung cancer): a randomized clinical trial. West Japan Study Group for lung cancer surgery (WJSG). *Eur J Cardiothorac Surg* 1999; **15**:438–443.

10 Fukuoka M, Yano S, Giaccone G, Tamura T, Nakagawa K, Douillard J-Y, *et al.* Multi-institutional randomized phase II trial of gefitinib for previously treated patients with advanced non-small-cell lung cancer. *J Clin Oncol* 2003; **21**:2237–2246.

11 Kris MG, Natale RB, Herbst RS, Lynch Jr TJ, Prager D, Belani CP, *et al.* Efficacy of gefitinib, an inhibitor of the epidermal growth factor receptor tyrosine kinase, in symptomatic patients with non-small cell lung cancer. A randomized trial. *J Am Med Ass* 2003; **290**:2149–2158.

12 Ochs J, Grous JJ, Warner KL. Final survival and safety results for 21,064 non-small-cell lung cancer (NSCLC) patients who received compassionate use gefitinib in a U.S. expanded access program (EAP). *Proc Am Soc Clin Oncol* 2004; **23**:628.

13 Onn A, Tsuboi M, Thatcher N. Treatment of non-small-cell lung cancer: a perspective on the recent advances and the experience with gefitinib. *Br J Cancer* 2004; **91(Suppl 2)**:S11–S17.

14 World Medical Association. World Medical Association Declaration of Helsinki. Recommendations guiding physicians in biomedical research involving human subjects. *J Am Med Ass* 1997; **277**:925–926.

15 Sato A, Toyoshima M, Kondo A, Ohta K, Sato H, Ohsumi A. Pneumonitis induced by the herbal medicine Sho-saiko-to in Japan. *Nihon Kyobu Shikkan Gakkai Zasshi* 1997; **35**:391–395.

16 Tohyama M, Tamaki Y, Toyama M, Ishimine T, Miyazato A, Nakamoto A, *et al.* A case of loxoprofen-induced pneumonitis pathologically resembling hypersensitivity pneumonitis. *Nihon Kokyuki Gakkai Zasshi* 2002; **40**: 123–128.

17 Miyazaki E, Ando M, Ih K, Matsumoto T, Kaneda K, Tsuda T. [Pulmonary edema associated with the Chinese medicine shosaikoto]. *Nihon Kokyuki Gakkai Zasshi* 1998; **36**:776–780.

18 Forsythe B, Faulkner K. Overview of the tolerability of gefitinib (IRESSA™) monotherapy. Clinical experience in non-small-cell lung cancer. *Drug Safety* 2004; **27**:1081–1092.

Locally Recurrent Central-Type Early Stage Lung Cancer < 1.0 cm in Diameter After Complete Remission by Photodynamic Therapy*

Kinya Furukawa, MD, PhD; Harubumi Kato, MD, PhD; Chimori Konaka, MD, PhD; Tetsuya Okunaka, MD, PhD; Jituo Usuda, MD, PhD; and Yoshiro Ebihara, MD, PhD

Background: **It is well known that central-type early stage lung cancer < 1.0 cm in diameter shows almost 100% complete response (CR) to photodynamic therapy (PDT). However, we have encountered cases of local recurrence after CR of tumors with a surface diameter < 1.0 cm.**
Patients and methods: **Ninety-three patients with 114 lesions were followed up, and cases of recurrence after CR has been obtained with initial tumors that had a diameter < 1.0 cm were examined. We compared the cytologic findings of local recurrence after CR to the cytologic findings before PDT. The relationship between the cell features and the depth of bronchial tumor invasion before PDT and on recurrence was evaluated.**
Results: **The CR and 5-year survival rates of patients with lesions < 1.0 cm were 92.8% (77 of 83 patients) and 57.9%, respectively; meanwhile, in the group of patients with lesions ≥ 1.0 cm, CR and 5-year survival rates were 58.1% (18 of 31 patients) and 59.3%. There was a significant difference in efficacy between the two groups ($p < 0.001$). Recurrences after CR were recognized in 9 of 77 lesions (11.7%) < 1.0 cm. When the recurrent tumor cells showed type I-II (low-to-moderate atypia) at the same site initially treated, CR could be obtained by a second PDT. Type III cells (high-grade atypia) showed the characteristics of tumor cells from deeper layers of the bronchial wall. Local recurrence at the same site may be caused by residual tumor cells from deep layers because of inadequate laser irradiation and penetration.**
Conclusions: **To reduce the recurrence rate, it is essential to accurately grasp the tumor extent and the depth of the bronchogenic carcinoma before performing PDT. Analysis of cell features of recurrent lesions after CR appears to be a useful source of information as to the depth of cancer invasion in the bronchial wall.** ***(CHEST 2005; 128:3269–3275)***

Key words: early stage lung cancer; occult lung cancer; photodynamic therapy; porfimer sodium

Abbreviations: AFB = autofluorescence bronchoscopy; CIS = carcinoma *in situ*; CR = complete remission; EBUS = endobronchial ultrasonography; ESLC = early stage lung cancer; PDT = photodynamic therapy; PR = partial remission

Lung cancer has a tendency to develop in older people, with a very poor prognosis. A total of 55,000 Japanese died from lung cancer in 2003, which made it the number-one cause of cancer death. Although diagnostic techniques such as high-resolution CT scan, video bronchoscopy, fluorescence bronchoscopy, and endobronchial ultrasonography (EBUS) have been developed recently, many patients with newly detected lung cancer still have inoperable advanced cancer. Therefore, the detection of early stage lung cancer (ESLC) is considered essential to reduce the mortality rate. Meanwhile, even when ESLC is detected, some cases are inoperable because of cardiopulmonary dysfunction due to age. Endoscopic procedures that are minimally invasive and do not compromise pulmonary function

*From the Department of Chest Surgery (Dr. Furukawa), Kasumigaura Hospital, Tokyo Medical University, Ibaraki; First Department of Surgery (Drs. Kato, Konaka, Usuda, and Ebihara), Second Department of Pathology, Tokyo Medical University, Tokyo; and Center for Respiratory Diseases (Dr. Okunaka), Sanno Hospital, Tokyo, Japan.
Manuscript received February 12, 2005; revision accepted May 9, 2005.

Correspondence to: Kinya Furukawa, MD, PhD, Department Chest Surgery, Tokyo Medical University, Kasumigaura Hospital, 3-20-1 Chuo, Ami-machi, Inashiki-gun, Ibaraki 300-0395, Japan; e-mail: k-furu@tokyo-med.ac.jp

are considered useful modalities for centrally located lung cancer. In particular, photodynamic therapy (PDT) is considered a useful and attractive modality for central-type ESLC.[1–7] Its action mechanism is considered to involve singlet oxygen, which is generated through photochemical reactions and causes degenerative necrosis of cells that have taken up the photosensitizer, *ie*, tumor cells.[8]

PDT using red laser light and a tumor-specific photosensitizer was established as a new therapeutic modality for central-type ESLC in 1982.[1] The length of longitudinal tumor extent was the only independent predictive factor for complete remission (CR), and 100% CR in lesions < 1.0 cm in diameter treated by PDT was reported.[5] However, we have encountered local recurrences after CR of tumor even in cases with a surface diameter < 1.0 cm. Therefore, we investigated the characteristics and cytomorphologic features of primary lesions and recurrences after CR in patients with lesions < 1.0 cm in diameter.

Materials and Methods

Patient Selection

A total number of 145 patients with 191 lesions of endoscopic ESLC underwent PDT from February 1980 to April 2001 in the Department of Tokyo Medical University. Of the 145 patients with 191 lesions, 93 patients with 114 lesions were followed up, and cases of recurrence after CR was obtained with initial tumors with a diameter < 1.0 cm were examined.

Procedures of PDT and Follow-up

The depth of tumor invasion was judged by biopsy specimen and CT scan, and was also evaluated by bronchoscopic findings based on the diagnostic criteria of ESLC defined by the Japan Lung Cancer Society.[9] To determine tumor size, bronchoscopic biopsies of the proximal and distal sites of the lesion and bronchoscopic measurements using forceps were performed. PDT procedures were performed with the combination of porfimer sodium (Photofrin; Wyeth Japan K.K.; Tokyo, Japan) that is taken up selectively in tumor, and an argon gas laser system (model 770; Spectra-Physics; Mountain View, CA) or excimer dye laser (EDL-1; Hamamatsu Photonics; Hamamatsu, Japan). Laser irradiation was performed via a quartz fiber inserted through the biopsy channel of the endoscope at 48 h after the IV administration of 2.0 mg/kg of porfimer sodium. The total energy of the laser irradiation was 100 J/cm^2, and energy levels in this range do not cause any heat degeneration or other adverse effects. The duration of irradiation required usually 10 to 20 min. Clean-up bronchoscopies to remove necrotic tissue produced by the PDT reaction were performed at 1, 3, and 7 days after PDT. Both cytologic and histologic examinations via fiberoptic bronchoscopy were performed at 1, 2, and 3 months, and thereafter at 3-month intervals in the first year and 6-month intervals after the second year until 5 years after PDT.

Efficacy Evaluation

The antitumor effect of initial treatment was rated based on endoscopic measurement of tumor size using forceps, morphologic observations, and histopathologic examination by biopsy, according to the general rules of the Japan Lung Cancer Society[9] and the Japan Society of Clinical Oncology.[10] The antitumor effect was rated at 1 month and 2 months after PDT. Antitumor effect was rated as CR (no demonstrable tumor microscopically by brushing and/or biopsy for a period of 4 weeks), partial remission (PR) [≥ 50% reduction in tumor size], no change (< 50% reduction or < 25% increase in tumor size), progressive disease (> 25% increase in tumor size), or not evaluable.

Evaluation of Cytomorphologic Features of Local Recurrences

In the central-type ESLC < 1.0 cm in greatest dimension, we have compared the cytologic findings of local recurrence after CR to the cytologic findings before PDT using bronchial brushing specimen. Cytologic findings were classified into three cytologic morphotypes using the classification of cell features proposed by Konaka and coworkers,[11] which appears to yield information as to the depth of cancer invasion in the bronchial wall. The classification was described as follows: type I cell, low-grade atypia (resembling atypical squamous cell metaplasia); type II cell, moderate-grade atypia (resembling early stage squamous cell carcinoma); and type III cell, high-grade atypia (resembling invasive squamous cell carcinoma). The biopsy specimens before PDT and on recurrence, or resected materials, in cases of resection after recurrence, were examined histopathologically, and the depth of bronchial wall invasion was classified into three groups: grade 1, carcinoma *in situ* (CIS) or microinvasion; grade 2, extramuscular bronchial wall invasion; and grade 3, intracartilaginous to extracartilaginous invasion. The relationship between the cell features and the depth of bronchial tumor invasion before and after PDT was evaluated.

Statistical Analysis

Statistical analysis were done using statistical software (Stat Flex for Windows, version 5.0; Artec; Osaka, Japan). The χ^2 test was used to compare the efficacy of PDT between lesions < 1.0 cm and > 1.0 cm in diameter. Differences between the survival rates of two groups in the Kaplan-Meier survival curves were analyzed using the log-rank test; $p < 0.05$ was considered to indicate a statistically significant difference.

Results

Results of PDT for Central-Type ESLC

A total of 93 patients with 114 lesions of central-type ESLC who underwent PDT were examined. Thirteen synchronous lesions in six cases, 15 metachronous lesions in six cases, and 5 synchronous/metachronous lesions in one case were observed. The evaluation of the efficacy of PDT is shown in Table 1. CRs and PRs were obtained in 75 patients with 95 lesions (83.3%) and in 18 patients with 19 lesions (16.7%) out of 93 patients with 114 lesions. Each lesion with PR was subsequently treated with other modalities, including surgery in 13 cases, chemotherapy in 5 cases, or radiotherapy in 1 case, and finally achieved 100% CR. Recurrences after CR were recognized in 12 of 95 lesions (12.6%). The 114 lesions were classified in two groups according to the

Table 1—*Results of PDT for Central-Type ESLC

Tumor Size, cm	Lesions, No.	CR	PR	Recurrence After CRT
< 1.0	83	77 (92.8)	6 (7.2)	9 (11.7)
≥ 1.0	31	18 (58.1)	13 (41.9)	3 (16.7)
Total	114	95 (83.3)	19 (16.7)	12 (12.6)

*Data are presented as No. (%) unless otherwise indicated.
†p < 0.001.

maximum longitudinal tumor extent. Of these, 83 lesions (72.8%) were < 1.0 cm and 31 lesions (27.2%) were ≥ 1.0 cm in diameter. The CR and PR rates in the group of patients with lesions < 1.0 cm in maximum diameter were 92.8% (77 of 83 patients) and 7.2% (6 of 83 patients), respectively. Meanwhile, in the group of patients with lesions ≥ 1.0 cm in diameter, the CR and PR rates were 58.1% (18 of 31 patients) and 41.9% (13 of 31 patients), respectively. Neither no change nor partial disease were observed in these groups. There was a significant difference in efficacy between the two groups using the χ^2 test ($p < 0.001$). Recurrences after CR were recognized in 9 of 77 lesions (11.7%) in the group < 1.0 cm and 3 of 18 lesions (16.7%) in the group ≥ 1.0 cm in diameter. The overall 5-year survival rates of the two groups were 57.9% and 59.3%, respectively (Fig. 1). There was no significant difference between the two groups on the basis of the log-rank test ($p = 0.207$).

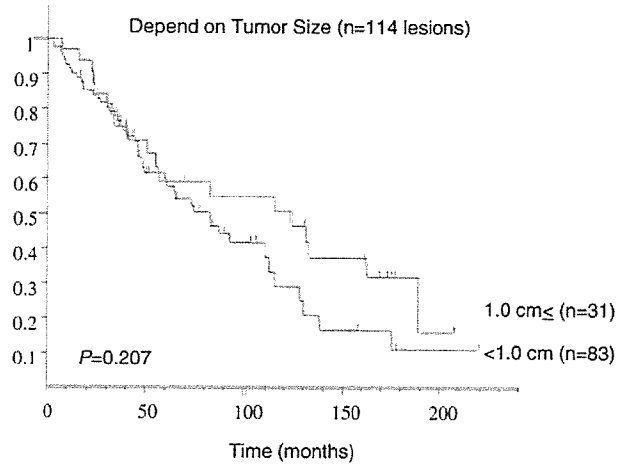

FIGURE 1. The overall 5-year survival rates were 57.9% in the group of patients with tumors < 1.0 cm and 59.3% in the group with tumors ≥ 1.0 cm in diameter, respectively. There was no significant difference between the survival rates of two groups in the Kaplan-Meier curves on the basis of the log-rank test ($p = 0.207$).

Characteristics of Local Recurrence < 1.0 cm in Diameter After CR

The information on nine patients with nine lesions in the group of patients with lesions < 1.0 cm in diameter who had recurrence after CR had been achieved by initial PDT are presented in Table 2. All patients with recurrence were male, and the age distribution ranged from 64 to 71 years (average age, 67.6 years at the time of initial diagnosis). Evidences of local recurrence were found in nine patients with nine lesions at the site of the primary lesion. The recurrent lesions were located on the trachea in one patient, lobar bronchus in one patient, segmental bronchi in five patients, and subsegmental bronchi in two patients. The average diameter of the nine recurrent lesions was 0.46 cm. All lesions were squamous cell carcinoma, and endoscopic findings showed nodular type in two lesions and superficial type in seven lesions. The disease-free interval of these nine patients ranged from 3 to 18 months (average, 10 months).

Local recurrence at site corresponding to the

Table 2—*Recurrent Cases After PDT for Central-Type ESLC < 1.0 cm in Diameter*

Case No.	Patient Age, yr	Lesion	Size, cm	BF Findings	CR, mo	Recurrence	Additional Treatment	Prognosis
1	66	Segmental bronchus rB^3	0.3	Superficial	18	PM	PDT, OP (RUL)	Alive (24 mo)
2	64	Subsegmental bronchus IB^3 a-b	0.3	Superficial	13	PM	PDT, OP (LPn)	Dead (56 mo), other disease
3	69	Subsegmental rB^{10} a-b	0.4	Superficial	10	PM	PDT Brachy	Alive (41 mo)
4	64	Segmental bronchus IB^{1+2}	0.6	Nodular	5	SS (CIS)	PDT	Alive (24 mo)
5	66	Segmental bronchus rB^1	0.5	Superficial	3	SS (CIS)		Dead (5 mo), other disease
6	69	Segmental bronchus IB^{1+2}	0.4	Superficial	14	SS (CIS)	PDT	Alive (27 mo)
7	71	Trachea	0.3	Nodular	10	SS (CIS)	PDT	Alive (27 mo)
8	70	Lobar bronchus rMid.-low	0.9	Superficial	6	SS (intracartilage)	OP (RML)	Dead (56 mo), other disease
9	69	Segmental IB^{1+2} B^3	0.4	Superficial	11	SS (extracartilage)	Nd-YAG, radiation, OP	Alive (65 mo)

*PM = peripheral margin initially treated; SS = same site initially treated; OP = operation; RML = right middle lobe; RUL = right upper lobe; LPn = left pneumonectomy; BF = bronchofiberscopic.

Table 3—*Cell Feature and Depth of Bronchial Invasion*

Case No.	Before PDT		Recurrence	
	Cytology (Brush) Type	Pathologic Grade	Cytology (Brush) Type	Pathologic Grade
4	I	1	I	1
5	I	1	I	1
6	I–II	1	I–II	1
7	I	1	II	1
8	I–II	1	II–III	3 (intracartilaginous invasion)
9	I	1	III	3 (extracartilaginous invasion)

peripheral margin of the lesion initially treated by PDT was observed in three patients (cases 1 to 3), while local recurrence at the same site as the initial tumor initially treated was observed in six patients (cases 4 to 9). The local recurrences at the site corresponding to the peripheral lesion were initially located in the subsegmental bronchus in two of three primary lesions. The patients with three local recurrences at the site corresponding to the peripheral margin underwent a second PDT session; however, CR was not obtained in any of these patients. Therefore, additional conventional surgery was performed in two patients and brachytherapy in one patient. The pathologic examinations of two operated patients showed residual tumor at the peripheral site. Right upper lobectomy was performed for case 1, and the resected material revealed superficial tumor invasion peripheral to the right B^3b. Left pneumonectomy was selected for case 2 (ipsilateral double cancer) because an ESLC was located at the bifurcation of left B^3a-b and a malignant lymphoma was in left B^6. This patient died due to malignant lymphoma at 56 months after the initial PDT session. Four patients (cases 4 to 7) with six local recurrences at the same site as the initial tumor local showed superficial tumor invasion (CIS), and a second PDT session was performed in three of four patients. CRs were again obtained in all three patients, who are presently disease free. One double cancer patient who had advanced stomach cancer underwent systemic chemotherapy without a second PDT but died 5 months after the initial PDT session. The pathologic examinations of the two other surgically treated patients (cases 8 and 9) revealed intracartilagious invasion of the bronchial wall. One multiple lung cancer patient (case 8) who received right middle and lower lobectomy after local recurrence died of hemoptysis due to another advanced lung cancer at 56 months after the initial PDT session. At the last follow-up of the nine patients who had local recurrence after CR had been obtained by initial PDT in whom the original primary lesion had been < 1.0 cm

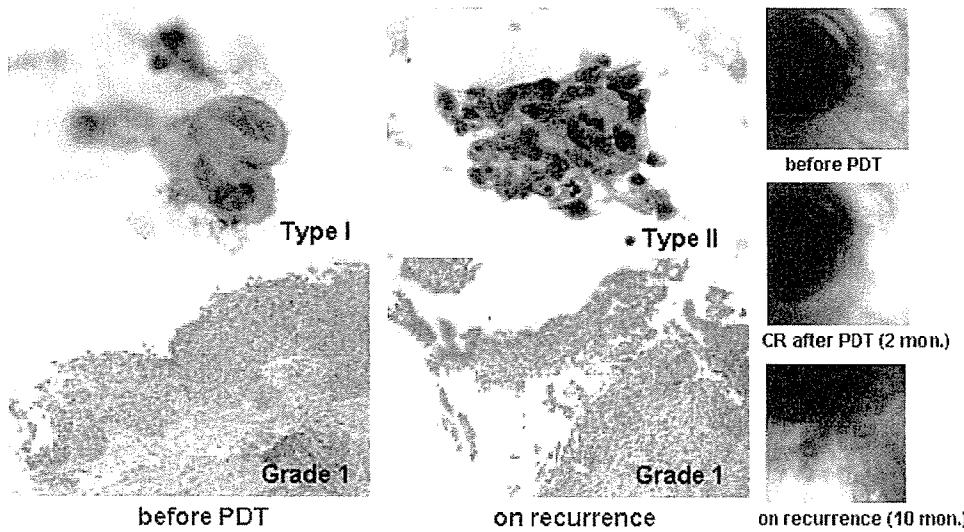

FIGURE 2. The cytopathologic and bronchoscopic findings in case 7. Bronchoscopic findings showed a small nodular tumor at the right side of the tracheal wall before PDT. Redness of the tracheal mucosa was observed on recurrence at 10 months after PDT. Cytologic findings before PDT were classified as type I because cell features showed a round shape and slight increase of nuclear chromatin but low-grade nuclear atypia. The biopsy specimen showed CIS (grade 1). Cytologic findings on recurrence were classified as type II because a sheet formation of polymorphic-shaped cells, increase of nuclear chromatin, and nuclear body were observed. Biopsy specimen on recurrence showed superficial tumor invasion (CIS) beneath the thin epithelial layer (grade 1). A second PDT was performed, and CR was again obtained in this patient.

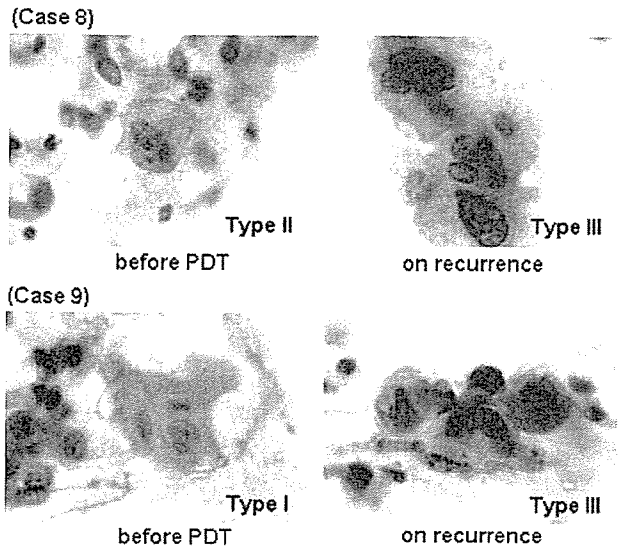

FIGURE 3. The findings of brushing cytology mainly observed in cases 8 and 9 before PDT and on recurrence after CR. Cytologic findings before PDT in case 8 were classified as type II because of a slight increase of nuclear chromatin. Cytologic findings before PDT in case 9 were classified as type I because of low-grade nuclear atypia. The findings of recurrent tumor cells in cases 8 and 9 were classified as type III because of severe increases of nuclear chromatin, high nuclear/cytoplasmic ratio, and high grade of nuclear atypia.

in diameter, three patients had died of other diseases and six patients were alive, and there were no deaths from the primary lesion.

Evaluation of Cytomorphologic Features of Local Recurrences

As mentioned above, local recurrence of the carcinoma at the same site as lesions < 1.0 cm in diameter initially treated successfully by PDT was observed in six out of nine locally recurrent patients (cases 4 to 9). A summary of the cell features and depth of bronchial wall invasion before PDT and after recurrence are shown in Table 3. The brushing cytology specimens before PDT mainly showed type I or II, and biopsy revealed grade 1 in all six cases. The majority of cell features in cases 4 to 7 showed type I or II, and the biopsy specimens showed grade 1 on recurrences. The cytopathologic and bronchoscopic findings of case 7 are shown Figure 2. Populations of type I and II cells were predominant in the recurrent lesions in these cases, which implied that the recurrent tumor was located in a superficial layer of bronchial wall. When the recurrent tumor cells showed type I-II (low-to-moderate atypia) local recurrence at the same site as the initial tumor initially treated, CR could be obtained by a second PDT. In cases 8 and 9, mainly type III cell features were observed in brushing cytology on recurrence (Fig 3). These two cases underwent resection, and the resected specimens revealed intracartilaginous tumor invasion of bronchial wall (grade 3), which implied the residual tumor located in a deep layer of bronchial wall.

DISCUSSION

PDT for cancer using a combination of low-power laser irradiation and tumor specific photosensitizer was first applied clinically by Dougherty et al[12] in 1978 to the skin metastasis of breast cancer. Since then, we performed the first reported endoscopic clinical application of PDT in cooperation with Dougherty and coworkers.[12] In Japan, PDT using porfimer sodium, a tumor-specific photosensitizer and excimer dye laser, was recognized by the government; and from April 1996, hospitals could receive reimbursement for PDT of early stage carcinomas of the lung, esophagus, stomach, and cervix from the national health insurance system.

The best PDT candidates in lung cancer are cases with central-type ESLC because of their endoscopic accessibility; therefore, selection of patient is important to achieve CR. Nagamoto et al[13] demonstrated that no lymph node involvement was found in 59 cancers with a longitudinal extent of < 20 mm; in another study,[14] histology by serial block sectioning showed that there was no nodal involvement in any CIS cases. Nakamura et al[15] retrospectively analyzed resected cases of central-type ESLC to clarify the relation between the endoscopic findings and the histologic extent of tumor. They demonstrated a significant difference is the maximum dimension according to the depth of bronchial invasion between CIS and extramuscular invasion and CIS and invasion into or beyond the cartilaginous layer. Lesions with a maximum diameter < 1.0 cm have a high possibility of being CIS. Their preoperative bronchoscopic diagnosis of centrally located ESLC was correct in 74.0%. In another study, Akaogi et al[16] demonstrated that polypoid or nodular lesions < 1.0 cm and flatly spreading lesions < 1.5 cm in greatest dimension were limited to within the cartilaginous layer without regional lymph node involvement. Also, Furuse et al[5] demonstrated that the length of longitudinal tumor extent was the only independent predictive factor for CR by PDT, and that lesions < 1.0 cm in diameter showed 100% CR. According to these data, therapy for CR requires satisfaction of the following endoscopic conditions: (1) no evidence of lymph node metastasis; (2) the lesion is superficial with a maximum diameter of < 1.0 cm; (3) no invasion into or beyond the cartilaginous layer; (4) the histologic type is squamous cell carcinoma; and

(5) the lesion is located in a position that can be easily irradiated with the laser.

In this study, excellent efficacy with a significant difference of CR rate was seen in patients with lesions < 1.0 cm (92.8%) compared to ≥ 1.0 cm (58.1%) in diameter; however, the overall 5-year survival rate of the two groups showed no significant difference (57.9% vs 59.3%). This may be because it was possible to perform additional alternative modalities such as surgery, second PDT, and brachytherapy to achieve CR after failure of initial PDT or recurrence after PDT. Considering that the 5-year survival rate of pathologic stage Ia (T1N0M0) patients who underwent surgery is approximately 67.0%,[17] our data are favorable because the majority of the PDT group consisted of patients with advanced age and poor cardiopulmonary function. Therefore, we consider that PDT may be used as first-line therapy for central-type ESLC prior to surgery, especially in cases with poor cardiopulmonary function. Also, Edell et al[18] and Cortese et al[19] demonstrated that PDT is an alternative to surgical resection in the management of early superficial squamous cell carcinoma.

In this study, recurrence after CR was recognized in 9 of 77 lesions (11.7%) in the group of patients with lesions < 1.0 cm in diameter. Despite the average diameter of the nine initial lesions being relatively small (0.46 cm), recurrence was recognized in eight of nine lesions (88.9%) within 12 months. Therefore, intensive follow-up studies should be performed until 1 year after PDT even for small primary lesions. The reasons why recurrences after CR were observed in the lesions < 1.0 cm in diameter could be explained by inappropriate estimation of the peripheral margin in cases of local recurrence at the site corresponding to the peripheral margin and insufficient laser irradiation or miss estimation of tumor depth in the cases of local recurrence at the same site as the initial tumor.

From our experiences, to achieve CR with PDT for central-type ESLC, it appears that not only the analysis of cell features but also the comprehension of tumor extent to the peripheral site and tumor invasion to the bronchial wall are of considerable significance. Kurimoto et al[20] demonstrated that endobronchial EBUS was useful to determine the depth of tumor invasion into the bronchial wall, and the accuracy of EBUS from the histopathologic findings was 95.8%. The EBUS image at 20 MHz shows five layers in the cartilaginous portion of bronchial wall. The third to fifth layers are images of cartilage. Therefore, it is feasible to evaluate the depth of invasion using EBUS whether or not the tumor invades into or beyond the cartilaginous layer.. In lesions with an intact third layer on EBUS, CR could be achieved with PDT. Miyazu et al[21] demonstrated that the depth of tumor invasion estimated by EBUS was accurate by histopathologic findings after surgical resection. They found 5 of 14 lesions (35.7%) < 1.0 cm in diameter that showed extracartilaginous invasion on the EBUS image that was later confirmed histopathologically; also, 3 of 5 lesions appeared bronchoscopically superficial but were shown to be extracartilaginous by EBUS. The indications of PDT for centrally located ESLC with a longitudinal extension of < 1.0 cm are unquestionable; meanwhile, we should realize that even < 1.0 cm in diameter can have extracartilaginous invasion. To comprehend the surface extent of superficial tumor invasion in the bronchial lumen, autofluorescence bronchoscopy (AFB) is considered useful.[22–25] The green autofluorescence of the lesion was decreased because of the lack of endogenous fluorophors, thickening of the membrane, and increased microvasculature.[26] We sometimes encountered unexpected surface invasion by AFB.

It is essential to know the extent of the tumor and the depth of bronchogenic carcinoma accurately for the selection of treatment modality. Corresponding to the previous study by Konaka et al,[11] the analysis of cell features is a useful source of information to evaluate the depth of cancer invasion in the bronchial wall. In addition, we believe that it could be beneficial information when choosing the treatment modality, such as recurrence after CR by PDT demonstrated in our study. Additionally, we now perform EBUS and AFB to determine the indications of PDT in all patients who have ESLC for the purpose of achieving 100% CR and reduction of recurrence rate. A comparative study of PDT for the treatment of ESLC before and after the adoption of EBUS and AFB will enable accurate evaluation of the benefits of these new diagnostic tools in the near future.

ACKNOWLEDGMENT: The authors are indebted to Professor J. P. Barron of the International Medical Communications Center of Tokyo Medical University for his review of this article.

References

1 Hayata Y, Kato H, Konaka C, et al. Hematoporphyrin derivative and laser photoradiation in the treatment of lung cancer. Chest 1982; 81:269–277

2 Kato H, Konaka C, Kawate N, et al. Five-year disease-free survival of a lung cancer patient treated only by photodynamic therapy. Chest 1986; 90:768–770

3 Edell ES, Cortese DA. Bronchoscopic phototherapy with hematoporphyrin derivative for treatment of localized bronchogenic carcinoma: a 5-year experience. Mayo Clin Proc 1987; 62:8–14

4 Edell ES, Cortese DA. Bronchoscopic localization and treatment of occult lung cancer. Chest 1989; 96:919–921

5 Furuse K, Fukuoka M, Kato H, et al. A prospective phase II

study on photodynamic therapy with Photofrin II for centrally located early-stage lung cancer. J Clin Oncol 1993; 11:1852–1187
6 Kato H. Photodynamic therapy for lung cancer: a review of 19 years' experience. J Photochem Photobiol 1998; B42:96–99
7 Kato H, Furukawa K, Sato M, et al. Phase II clinical study of photodynamic therapy using mono-L-aspartyl chlorin e6 and diode laser for early superficial squamous cell carcinoma of the lung. Lung Cancer 2003; 42:103–111
8 Niedre M, Patterson MS, Wilson BC. Direct near-infrared luminescence detection of singlet oxygen generated by photodynamic therapy in cells *in vitro* and tissues *in vivo*. Photochem Photobiol 2002; 75:382–391
9 General rules for clinical and pathological records of lung cancer. 4th ed. In: Japan Lung Cancer Society, eds. Tokyo, Japan: Kanehara and Company, 1995; 123–133
10 Niiya H. Toxicity grading criteria of the Japan Clinical Oncology Group. Int J Clin Oncol 1997; 32:61–65
11 Konaka C, Miura H, Ikeda N, et al. The characteristics of early bronchogenic carcinoma evaluated by cytomorphological features. Lung Cancer 2002; 38:267–271
12 Dougherty TJ, Lawrence G, Kaufman JH, et al. Photoradiation in the treatment of recurrent breast carcinoma. J Natl Cancer Inst 1978; 62:231–237
13 Nagamoto N, Saito Y, Ohta S, et al. Relationship of lymph node metastasis to primary tumor size and microscopic appearance of roentgenographically occult lung cancer. Am J Surg Pathol 1989; 13:1009–1013
14 Nagamoto N, Saito Y, Sato M, et al. Clinicopathological analysis of 19 cases of isolated carcinoma in situ of the bronchus. Am J Surg Pathol 1993; 17:1234–1243
15 Nakamura H, Kawasaki N, Hagiwara M, et al. Endoscopic evaluation of centrally located early squamous cell carcinoma of the lung. Cancer 2001; 91:1142–1147
16 Akaogi E, Ogawa I, Mitsui K, et al. Endoscopic criteria of early squamous cell carcinoma of the bronchus. Cancer 1994; 74:3113–3117
17 Mountain CF. Revisions in the international system for staging lung cancer. Chest 1997; 111:1710–1717
18 Edell ES, Cortese DA. Photodynamic therapy in the management of early superficial squamous cell carcinoma as an alternative to surgical resection. Chest 1992; 102:1319–1322
19 Cortese DA, Edell ES, Kinsey JH. Photodynamic therapy for early stage squamous cell carcinoma of the lung. Mayo Clin Proc 1997; 72:595–602
20 Kurimoto N, Murayama M, Yoshioka S, et al. Assessment of usefulness of endobronchial ultrasonography in determination of depth of tracheobronchial tumor invasion. Chest 1999; 115:1500–1506
21 Miyazu Y, Miyazawa T, Kurimoto N, et al. Endobronchial ultrasonography in the assessment of centrally located early-stage lung cancer before photodynamic therapy. Am J Respir Crit Care Med 2002; 165:832–837
22 Lam S, Kennedy T, Unger M, et al. Localization of bronchial intraepithelial neoplastic lesions by fluorescence bronchoscopy. Chest 1998; 113:696–702
23 Ikeda N, Hiyoshi T, Kakihana M, et al. Histopathological evaluation of fluorescence bronchoscopy using resected lungs in cases of lung cancer. Lung Cancer 2003; 41:303–309
24 Sutedja TG, Codrington H, Risse EK, et al. Autofluorescence bronchoscopy improves staging of radiographically occult lung cancer and has an impact on therapeutic strategy. Chest 2001; 120:1327–1332
25 Sutedja TG, Venmans BJ, Smit EF, et al. Fluorescence bronchoscopy for early detection of lung cancer: a clinical perspective. Lung Cancer 2001; 34:157–168
26 Furukawa K, Ikeda N, Miura T, et al. Is autofluorescence bronchoscopy needed to diagnose early bronchogenic carcinoma? J Bronchol 2003; 10:64–69

Systemic Antitumor Effect of Intratumoral Injection of Dendritic Cells in Combination with Local Photodynamic Therapy

Hisashi Saji,[1,3] Wenru Song,[2] Katsuyoshi Furumoto,[1] Harubumi Kato,[3] and Edgar G. Engleman[1]

Abstract

Purpose: Photodynamic therapy (PDT), which is used clinically for the palliative treatment of cancer, induces local tumor cell death but has no effect on tumors in untreated sites. The purpose of this study was to determine if local PDT followed by intratumoral injection of naïve dendritic cells (IT-DC) induces systemic antitumor immunity that can inhibit the growth of untreated as well as PDT + IT-DC – treated tumors.

Experimental Design: BALB/c or C57Bl/6 mice were injected s.c. with CT26 colorectal carcinoma cells and B16 melanoma cells, respectively, and following 10 to 12 days of tumor growth, the tumors were treated with PDT alone or PDT followed by IT-DC or IT-PBS. In other studies, tumors were established simultaneously in both lower flanks or in one flank and in the lungs, but only one flank was treated.

Results: Whereas neither PDT nor IT-DC alone was effective, PDT + IT-DC eradicated both CT26 and B16 tumors in a significant proportion of animals and prolonged the survival of mice of which the tumors were not cured. The spleens of mice treated with PDT + IT-DC contained tumor-specific cytotoxic and IFN-γ-secreting T cells whereas the spleens of control groups did not. Moreover, adoptive transfer of splenocytes from successfully treated CT26 tumor-free mice protected naïve animals from a subsequent challenge with CT26, and this was mediated mainly by CD8 T cells. Most importantly, PDT plus IT-DC administered to one tumor site led to tumor regression at distant sites, including multiple lung metastases.

Conclusions: PDT + IT-DC induces potent systemic antitumor immunity in mice and should be evaluated in the treatment of human cancer.

Dendritic cells (DC) are the most potent antigen-presenting cells known, uniquely capable of activating both the cognate and innate arms of the immune system. For example, administration of DCs loaded *ex vivo* with tumor-associated antigens can elicit antitumor immunity resulting in tumor regression in various murine models, and DCs pulsed with tumor derived peptides, proteins, genes or lysates, as well as DCs fused with tumor cells, have all been studied as therapeutic cancer vaccines (1–11). Although the methods are complex and costly to implement, promising results have been obtained in clinical trials in patients with advanced malignancies. These trials have shown DC-based vaccination to be well tolerated and capable of inducing tumor-specific T-cell responses and regression of metastatic disease. On the other hand, the overall therapeutic efficacy of this approach has been limited, indicating a need to either enhance its potency or combine it with other treatment modalities.

Among the modalities that might be combined with DC-based immunotherapy are systemically administered antitumor drugs as well as locally targeted therapies such as radiation, radiofrequency ablation, and photodynamic therapy (PDT). PDT has been approved in the United States and other countries as an anticancer therapy, mainly for the palliative treatment of surgically inaccessible tumors. PDT involves the systemic administration of a photosensitizer that preferentially accumulates in transformed cells, followed by illumination of the tumor with a laser beam (12). In the presence of oxygen, the laser light activates the photosensitizer and initiates a complex photochemical reaction that generates cytotoxic intermediates. Tumor destruction after PDT results from direct cytotoxic effects as well as from the induction of a local inflammatory response (12). Thus, preclinical studies have shown that PDT not only mediates apoptotic and necrotic killing of tumor cells but also alters the tumor microenvironment through the release of proinflammatory cytokines such as tumor necrosis factor α, interleukin (IL)-1 and IL-6 (12, 13).

On the basis of its unique mechanism of tumor destruction, PDT has the potential to create an environment at the tumor site that favors both tumor antigen loading and activation of DCs, key requirements for induction of antitumor immunity (14). Because most tumors lack an abundance of DCs, one way to potentially take advantage of this environment would be to inject a sufficient number of autologous DCs directly into

Authors' Affiliations: Departments of [1]Pathology and [2]Medicine, Stanford University School of Medicine, Palo Alto, California and [3]Department of Surgery, Tokyo Medical University, Tokyo, Japan

Received 9/12/05; revised 1/5/06; accepted 1/19/06.

Grant support: National Heart, Lung, and Blood Institute grant HL57443 (E.G. Engleman) and NIH National Cancer Institute grant K08CA105064 (W. Song).

The costs of publication of this article were defrayed in part by the payment of page charges. This article must therefore be hereby marked *advertisement* in accordance with 18 U.S.C. Section 1734 solely to indicate this fact.

Note: H. Saji and W. Song contributed equally to this work.

Requests for reprints: Edgar G. Engleman, Stanford Blood Center, 3373 Hillview Avenue, Palo Alto, CA 94304-1204. Phone: 650-723-7960; Fax: 650-725-0592; E-mail: edengleman@stanford.edu.

doi:10.1158/1078-0432.CCR-05-1986

PDT-treated tumors. Such a strategy alleviates the need to do *in vitro* loading of DCs with tumor antigens because the inflammatory milieu induces DC activation, which facilitates not only antigen acquisition and processing but also migration of the DCs to draining lymph nodes where they interact with a broad range of potential effector cells. In the current study, we evaluated the effect of combining PDT with intratumoral injection of syngeneic DCs (IT-DC) on two histologically distinct murine tumors, CT26 colon carcinoma and B16 melanoma. The results show that this combined treatment induces strong and durable tumor-specific immunity that results in the destruction not only of targeted tumors but also of tumors at distant sites.

Materials and Methods

Mice. Female BALB/c (H-2^d) and C57Bl/6 (H-2^b) mice, 6 to 8 weeks of age, were purchased from The Jackson Laboratory (Bar Harbor, ME). All mice were housed in the Stanford animal facility in accordance with the NIH guidelines.

Cell lines. The murine CT26 colon carcinoma, B16 melanoma (F10 clone), MAD109 lung carcinoma, and EL-4 lymphoma cell lines used in this study were maintained in complete RPMI 1640 with 10% fetal bovine serum, penicillin G (100 units/mL), streptomycin (100 μg/mL), and L-glutamine (10 mmol/L).

DCs. Bone marrow–derived DCs were generated in the presence of granulocyte macrophage colony-stimulating factor and IL-4 for 7 days as previously described (15). Bone marrow cells were harvested from femurs and tibias, and after RBC lysis, the resulting cell suspension was incubated in complete RPMI 1640 containing recombinant murine granulocyte macrophage colony-stimulating factor (10 ng/mL; PeproTech, Inc., Rocky Hill, NJ) and recombinant murine IL-4 (10 ng/mL; PeproTech). On day 2, nonadherent granulocytes were gently removed and fresh medium with granulocyte macrophage colony-stimulating factor and IL-4 was added. On day 5, loosely adherent cells were dislodged and replated. On day 7 of culture, the unpulsed DCs were collected. The maturational status and percentage of DCs were verified by flow cytometry, and staining of three surface markers (CD11c, CD86, and class II antigen) showed the purity of DCs to be ≥74%.

Photosensitizer and laser unit. ATX-S10 Na(II), a hydrophilic chlorin photosensitizer with an absorption maximum at 670 nm (16), was obtained from Photochemical Co. Ltd. (Okayama, Japan). A diode laser (Hamamatsu Photonics, Hamamatsu, Japan) was used as a light source for exciting ATX-S10 Na(II). The diode laser is a continuous-wave laser operating at 670-nm wavelength.

During the light irradiation, mice were anesthetized with ketamine (125 mg/kg: Vedco, Inc., St. Joseph, MO) and xylazine (25 mg/kg; Phoenix Pharmaceutical, Inc., St. Joseph, MO) and were restrained in a specially designed holder.

Combined PDT and IT-DC therapy of CT26 colon cancer. Preliminary studies with ATX-S10 Na(II) and a diode laser, were carried out on the basis of a published protocol (16) to identify a drug dose and laser setting for inhibition of growth of CT26 tumors *in vivo* without major local or systemic toxicity. CT26 tumor cells (10^6 per mouse) in 100 μL HBSS were injected into the lower right flank of BALB/c mice. On day 12, when the average tumor volume was 153.0 ± 11.5 mm^3, the mice received an i.v. injection of ATX-S10 Na(II) (5 mg/kg body weight), followed 4 to 5 hours later by 150 J/cm^2 laser irradiation of the tumor. DCs (1×10^6 per injection in 50 μL PBS) were injected into the tumor on days 13, 14, 15, and 17. The tumor volume was measured thrice a week using a caliper [tumor volume (mm^3) = (longer diameter) × (shorter diameter)^2 × 0.4]. Animals were sacrificed when the tumor diameter exceeded 20 mm or when there were signs of animal distress. Survival was recorded as the percentage of surviving animals on a given day. Surviving mice had no sign of tumor when experiments were terminated.

Combined PDT and IT-DC therapy of B16 melanoma. For the B16 melanoma tumor model, C57Bl/6 mice were inoculated s.c. with 5×10^5 tumor cells in the lower right flank. On day 10, mice with established tumors (average tumor volume, 80.0 ± 5.4 mm^3) were treated with 150 J/cm^2 laser irradiation to the tumor 4 to 5 hours after an ATX-S10 Na(II) (5 mg/kg body weight) injection and given intratumoral injections of DCs on days 11, 12, 13, and 15 (1×10^6 per injection in 50 μL PBS). The measurement of tumor volume and survival was as above.

ELISPOT assays. ELISPOT assays were done with an ELISpot mouse IFN-γ system (R&D Systems, Inc., Minneapolis, MN) according to the instructions of the manufacturer. Splenocytes were isolated 4 weeks after tumor inoculation. After lysis of RBC, splenocytes were resuspended at a final concentration of 5×10^5/mL and 100 μL of this suspension were then incubated at 37°C for 24 hours in ELISPOT plates coated with anti-IFN-γ with 100 μL medium with or without irradiated (30 Gy) stimulator cells (CT26, MAD109, B16, or EL-4).

Cytotoxicity assays. Cytotoxicity was measured by a standard chromium-51(^{51}Cr) release assay. Splenocytes were harvested 4 weeks after tumor inoculation. After lysis of RBC, splenocytes (1×10^6/mL) were stimulated *in vitro* by irradiated (100 Gy) tumor cells (1×10^5/mL) at 37°C for 5 days in the presence of 10 units/mL IL-2. Following culture, splenocytes were separated from dead cells and debris with Lympholyte-M cell separation media (Cederlane Laboratories, Inc., Hornby, Ontario, Canada). Target cells were labeled with ^{51}Cr (200 μCi/5×10^6 cells) for 1 hour at 37°C, washed, and then incubated in U-bottomed wells with effector cells at various effector-to-target cell ratios at 37°C for 4 hours. Spontaneous release and maximum release were determined by incubating target cells in medium alone or in 1% SDS, respectively. Spontaneous release was always <20% of maximum. Radioactivity was counted in a liquid scintillation counter and the percentage of specific target cell lysis was calculated with the formula $[(E - S) / (T - S)] \times 100$, where E is the average experimental release, S is the average spontaneous release, and T is the average maximal release.

Adoptive transfer of splenocytes. To determine whether lymphocytes induced by PDT + IT-DC could protect naïve animals from a tumor challenge, BALB/c mice were inoculated s.c. with CT26 cells and treated with PDT + IT-DC as before. Four weeks later, the splenocytes were harvested and 1×10^7 cells were infused i.v. into naïve mice. Control groups of mice received splenocytes from CT26 tumor-bearing mice treated with either IT-PBS alone, IT-DC alone, or PDT + IT-PBS. One day later, these mice were s.c. challenged with a lethal number (1×10^6) of CT26 cells and monitored for tumor volume and survival.

To analyze the role of specific T-cell subsets in tumor protection, splenocytes were harvested from inoculated tumor-free mice treated with PDT + IT-DC, and $CD4^+$ or $CD8^+$ T cells were depleted by using CD4 (L3T4) or CD8a (Ly-2) coupled microbeads and magnetic cell sorting (Miltenyi Biotec, Inc., Auburn, CA). Splenocytes, $CD4^+$ T-cell–depleted splenocytes, or $CD8^+$ T-cell–depleted splenocytes (1×10^7) were infused i.v. into groups of five naïve mice. Control mice received splenocytes from naïve mice. One day later, the mice were s.c. challenged with a lethal number (1×10^6) of CT26 cells and monitored for tumor volume and survival. These depletion conditions were validated by flow cytometry analysis using anti-CD4 (L3T4)-FITC and CD8a (Ly-2)-phycoerythrin monoclonal antibodies (PharMingen, San Diego, CA). The percent depletion of $CD4^+$ and $CD8^+$ cells was 97% and 93%, respectively.

Secondary tumor challenge. To determine the persistence of tumor-specific immunity in the mice treated by PDT + IT-DC, at day 60 after first tumor inoculation, mice showing complete regression of CT26 tumors were given a second s.c. tumor challenge (1×10^6 CT26) in the left lower flank (contralateral to the first injection site). These mice, as well as a control group of naïve mice that were inoculated with 1×10^6 CT26 tumor cells, were monitored for tumor size and survival.

Effect of PDT + IT-DC on contralateral tumors. To determine whether PDT + IT-DC treatment of one s.c. tumor affected an

established contralateral s.c. tumor, CT26 cells (1×10^6) were injected s.c. into both lower flanks of BALB/c mice on day 0. On day 12, tumor-bearing mice were either untreated or treated with combined PDT + IT-DC (using the protocol above) into the tumor on the right side but not into the tumor on the left side. The bilateral tumor-bearing mice were followed for tumor volume on both flanks.

Effect of PDT + IT-DC on multiple distant tumors. BALB/c mice were inoculated s.c. with 1×10^6 CT26 tumor cells on day 0. On day 5, these mice were injected i.v. with 1×10^6 CT26 tumor cells. PDT + IT-DC was administered on day 12 (as above) to the s.c. tumor alone. On day 21 after i.v. tumor inoculation, mice were euthanized and lungs were harvested and fixed with Bouin's solution (Sigma-Aldrich, St. Louis, MO).

Statistical analysis. Differences between groups were analyzed using unpaired two-tailed Student's *t* test. Survival curves were plotted by the Kaplan-Meier method and comparisons among groups in the survival data were calculated by log-rank test.

Results

Effect of combination treatment with PDT and IT-DC on CT26 tumors. To test the hypothesis that local PDT followed by IT-DC can inhibit primary tumor growth, BALB/c mice were injected s.c. with CT26 tumor cells. On day 12, the tumors reached an average diameter of 10.5 mm and could not be cured with PDT alone (data not shown). PDT was done at that time and syngeneic DCs were injected intratumorally 1 day later (day 13) and again on days 14, 15, and 17. Although the tumors grew rapidly following treatment with PBS alone, IT-DC alone, and PDT + IT-PBS, the combination of PDT + IT-DC resulted in significant suppression of tumor growth ($P < 0.05$ versus all other groups; Fig. 1A). Four of the nine (44%) animals treated with PDT + IT-DC became tumor-free and the overall survival of the PDT + IT-DC group was significantly prolonged compared with other groups (log-rank test, $P = 0.0006$; Fig. 1B). To determine if the combination of PDT + IT-DC results in immunologic memory, mice that had been treated with PDT + IT-DC and were tumor-free following an initial tumor inoculation were rechallenged in the opposite flank with a second lethal inoculation of the same tumor. The results show that these mice not only survived but were completely resistant to this second inoculation (Fig. 1C).

Effect of combination treatment with PDT and IT-DC on B16 tumors. In contrast to CT26 tumors, the B16 melanoma is considered poorly immunogenic and highly aggressive. Moreover, PDT for the treatment of melanoma has had only limited benefit (17), which is attributed to the presence in such tumors of a large amount of light-absorbing melanin pigment that prevents penetration of the laser beam into the tumor tissue. Our preliminary studies showed that PDT alone could not induce any suppression of growth of B16 tumors, even against s.c. tumors as small as 3 mm in diameter (data not shown). Surprisingly, PDT in combination with IT-DC resulted in a striking antitumor effect ($P < 0.05$, versus all other groups; Fig. 2A). Four of seven (57%) mice treated with PDT + IT-DC became tumor-free and the overall survival of the PDT + IT-DC group was significantly prolonged compared with other groups (log-rank test, $P = 0.0004$; Fig. 2B). Interestingly, two of four PDT + IT-DC–treated tumor-free mice developed white hair at sites of treatment, and in one of these mice, white hair could be seen at a site (neck) distant from the PDT site at ~40 days after treatment (Fig. 2C).

In vitro characterization of the antitumor immune response induced by PDT + IT-DC. A correlation between *in vitro* tumor-specific IFN-γ production by host-derived T cells and systemic antitumor immunity has been shown in other studies (18, 19). Using ELISPOT assays, we evaluated whether treatment of CT26 tumor-bearing mice with PDT + IT-DC could elicit tumor-specific IFN-γ-secreting T cells. As shown in Fig. 3A, splenocytes from mice treated with PDT + IT-DC contained significantly more tumor-specific IFN-γ-secreting cells than splenocytes from other groups ($P < 0.05$, versus other groups). Moreover, this cytokine was not secreted spontaneously or in response to

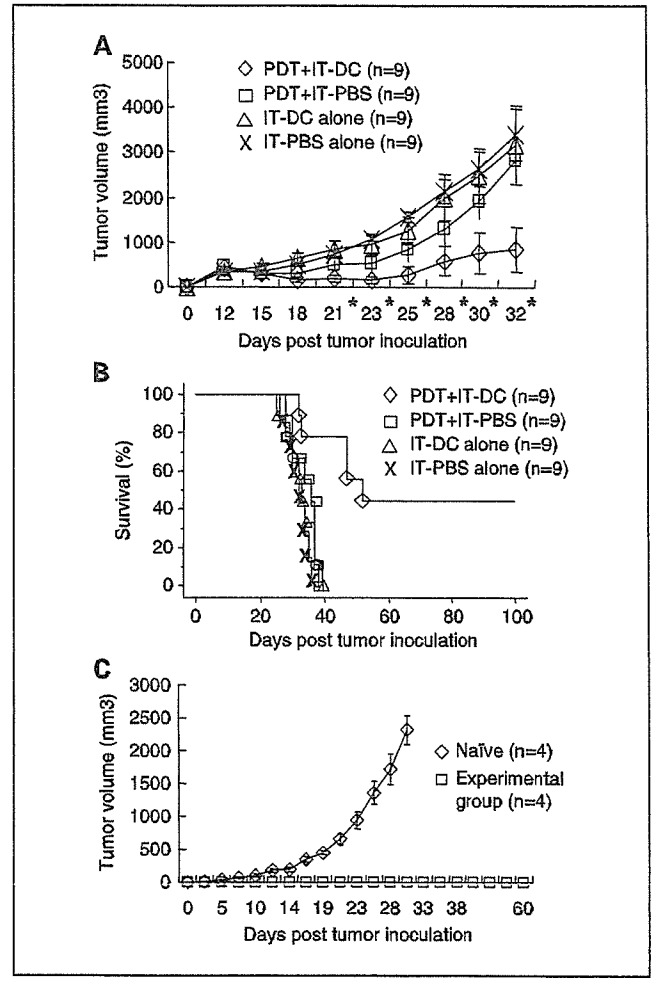

Fig. 1. Effect of combined PDT + IT-DC on the growth of established CT26 syngeneic colon carcinoma tumors. CT26 cells (1×10^6) were injected s.c. in the right lower flank of BALB/c mice. On day 12, mice with established tumors (mean tumor volume 153.0 ± 11.5 mm^3) were treated with PDT as described in Materials and Methods. DCs (1×10^6 in 50 μL PBS) were administered intratumorally on days 13, 14, 15, and 17. The experimental groups included intratumoral injection of PBS alone (50 μL, $n = 9$; ×); intratumoral injection of DCs alone ($n = 9$; △); PDT combined with intratumoral PBS ($n = 9$; □); and PDT combined with IT-DC ($n = 9$; ◇). *A*, mean tumor volume (mm^3) for treatment groups [mean tumor volume = (longer diameter) × (shorter diameter)^2 × 0.4]. Points, mean; bars, SE. *, $P < 0.05$, PDT + IT-DC versus other treatments. *B*, survival of mice recorded as the percentage of surviving animals on a given day. Surviving mice had no sign of tumor when the experiment was terminated. *C*, CT26 tumor rechallenge of tumor-free mice after PDT + IT-DC. Mice that had received CT26 inoculation followed by PDT + IT-DC were rechallenged s.c. with a lethal number (1×10^6) of CT26 tumor cells ($n = 4$; □). Naïve mice inoculated s.c. with the same number of CT26 cells served as controls ($n = 4$; ◇). Experiments were done thrice with similar results.

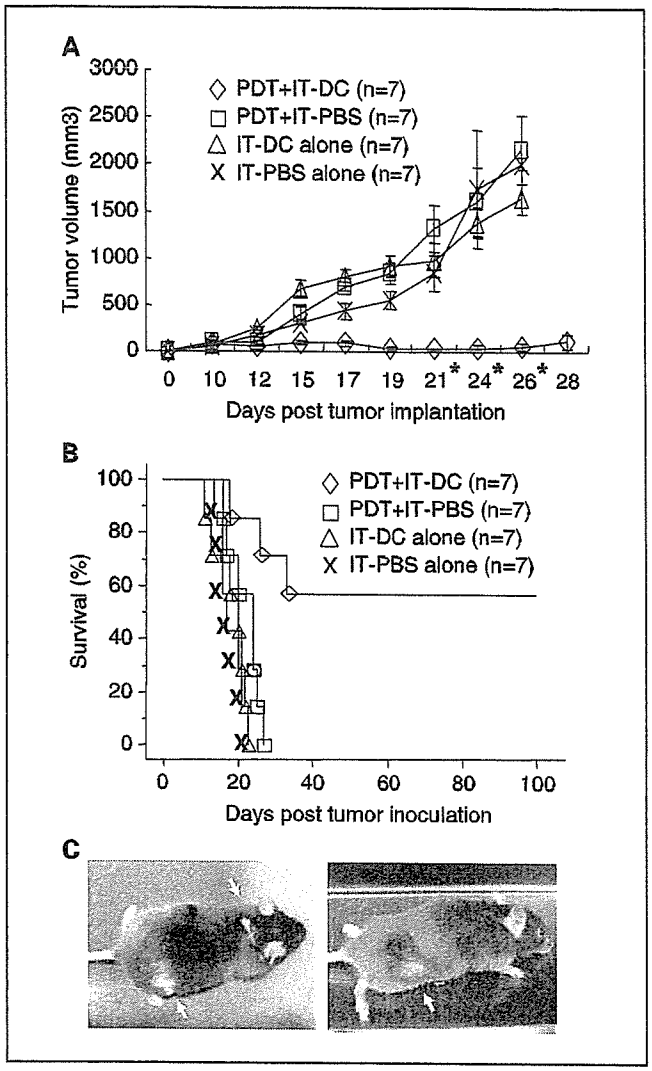

Fig. 2. Effect of PDT + IT-DC on the growth of established B16 melanoma tumors. B16 cells (5×10^5) were injected s.c. in the right lower flank of C57Bl/6 mice. On day 10, mice with established tumors (average tumor size, 80.0 ± 5.4 mm^3) were treated with PDTand received IT-DC (1×10^6 in 50 μL PBS) on days 11, 12, 13, and 15. The experimental groups included IT-PBS alone (50 μL, $n = 7$; ×); IT-DC alone ($n = 7$; △); PDT + IT-PBS ($n = 7$; □); and PDT + IT-DC ($n = 7$; ◇). *A*, mean tumor volume (mm^3) for treatment groups [mean tumor volume = (longer diameter) × (shorter diameter)^2 × 0.4]. Points, mean; bars, SE. *, $P < 0.05$, PDT + IT-DC versus other treatments. *B*, survival of mice recorded as the percentage of surviving animals on a given day. Surviving mice had no sign of tumor when the experiment was terminated. Experiments were done thrice with similar results. *C*, photographs of tumor-free mice taken 60 days after PDT + IT-DC treatment of B16 melanoma. Arrows, white hair growing in an untreated site (neck of mouse on left) and in treated sites (right flanks of both mice).

MAD109 cells, which are irrelevant syngeneic murine lung tumor cells, indicating that the observed response was immunologically specific to CT26 tumor cells. In additional studies, we analyzed the splenocytes of the different treatment groups for the presence of CT26-specific CTLs. Figure 3B shows that such cells were present in the PDT + IT-DC group but not in other groups ($P < 0.05$, versus all other groups). There was no killing of a syngeneic lung cancer cell line (MAD109), indicating that the CTLs are CT26 tumor specific (data not shown).

A tumor-specific immune response was also observed in B16 tumor-bearing mice that had been treated with PDT + IT-DC. As shown in Fig. 4A, splenocytes from such mice contained significantly more tumor-specific IFN-γ-secreting cells compared with splenocytes from control groups ($P < 0.05$). In addition, as shown in Fig. 4B, PDT + IT-DC induced tumor-specific CTLs, as indicated by the presence of such cells in treated but not control animals. No lysis of a syngeneic lymphoma cell line (EL-4) was observed, indicating those CTLs are B16 tumor specific (data not shown).

In vivo *characterization of the antitumor immune response induced by PDT + IT-DC.* To further evaluate the role of CTLs in PDT + IT-DC–induced tumor protection, splenocytes from CT26 inoculated PDT + IT-DC–treated tumor-free mice and splenocytes from control groups were transferred to naïve mice. One day later, the mice were inoculated with a lethal dose of

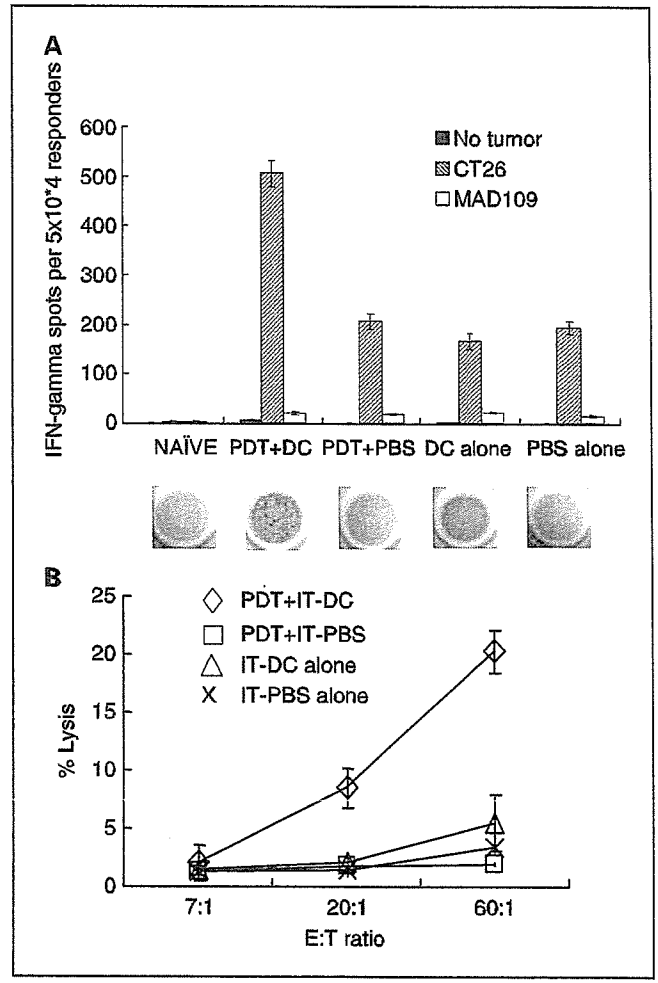

Fig. 3. Induction of *in vitro* anti-CT26 tumor immunity by PDT + IT-DC. *A*, CT26 tumor-bearing mice were treated as detailed in the legend to Fig. 1. Four weeks after tumor inoculation, splenocytes from treated, control, and naïve mice were incubated with or without specific tumor cells or MAD109, irrelevant irradiated tumor cells in an IFN-γ ELISPOTassay. Columns, average number of spots per 5×10^4 responders of triplicate samples; bars, SE. *, $P < 0.05$, versus other groups. Representative ELISPOT wells are shown below the graph. Data are from one of three representative experiments. *B*, CTLs in mice that had been inoculated with CT26 tumor cells followed by treatment with PDT + IT-DC. Four weeks after tumor inoculation, graded numbers of splenocytes from mice receiving various treatment protocols (×, IT-PBS alone; △, IT-DC alone; □, PDT + IT-PBS; ◇, PDT + IT-DC) were cultured in the presence of irradiated CT26 cells for 5 days. Cytotoxicity was measured with a standard 4-hour ^{51}Cr release assay at various ratios of effectors to targets using ^{51}Cr-labeled CT26 cells as targets.

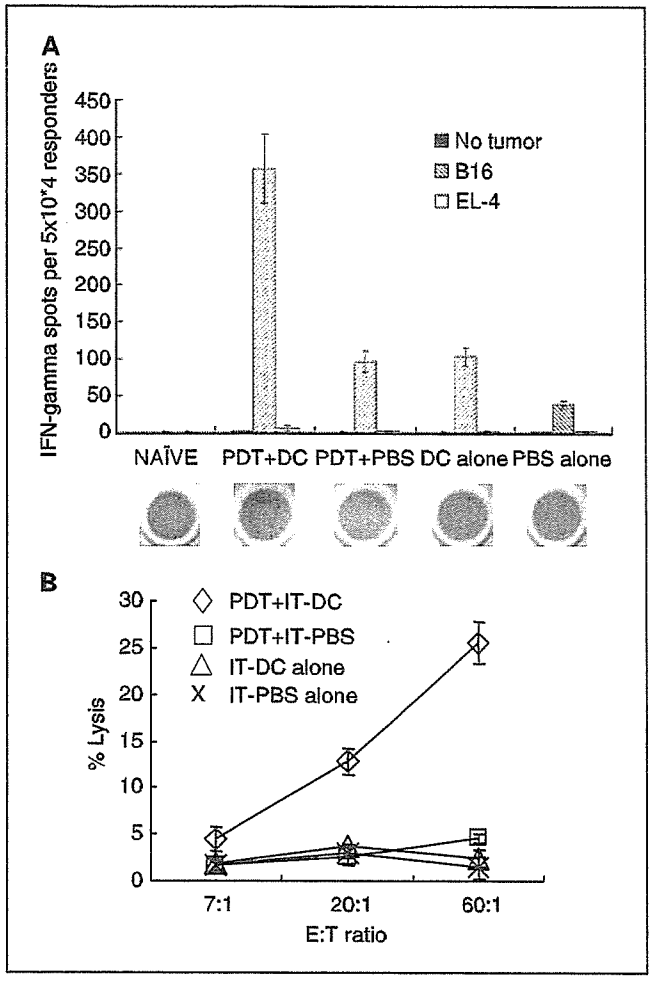

Fig. 4. Induction of anti-B16 tumor immunity by PDT + IT-DC treatment. *A*, B16 tumor–bearing mice were treated as detailed in the legend to Fig. 2. Four weeks after tumor inoculation, splenocytes from treated, control, and naive mice were incubated with or without specific target cells or irrelevant irradiated tumor cells (EL-4) in an IFN-γ ELISPOT assay. Columns, average number of spots per 5×10^4 responders of triplicate samples; bars, SE. *, $P < 0.05$, versus other groups. Representative wells from an ELISPOT plate are shown below the graph. Data are from one of three representative experiments. *B*, CTLs in mice that received B16 tumor inoculation followed by treatment with PDT + IT-DC. Four weeks after tumor inoculation, graded numbers of splenocytes were cultured in the presence of irradiated B16 tumor cells for 5 days (×, IT-PBS alone; △, IT-DC alone; □, PDT + IT-PBS; ◇, PDT + IT-DC). Cytotoxicity was measured with a 4-hour ^{51}Cr release assay at various ratios of effectors to targets using ^{51}Cr-labeled B16 cells as targets.

CT26 tumor cells. Mice receiving splenocytes from the PDT + IT-DC–treated mice, but not from other mice, were protected from a subsequent tumor challenge with CT26 (Fig. 5A). To determine the role of $CD4^+$ and $CD8^+$ T cells in tumor protection, we repeated this experiment using whole splenocytes or splenocytes depleted of $CD4^+$ or $CD8^+$ T cells. Splenocytes from naïve mice were used as negative controls. One day later, these mice were s.c. challenged with a lethal number of CT26 tumor cells. As shown in Fig. 5B, whereas both $CD4^+$ and $CD8^+$ T cells from PDT + IT-DC–treated mice contributed to tumor protection, CD8 T cells mediated most of the effect.

Effect of PDT + IT-DC on distant untreated tumors. To determine whether treatment of one tumor with PDT + IT-DC conferred systemic antitumor effects, CT26 tumors were established simultaneously in both lower flanks, but only one site was treated with PDT + IT-DC. As shown in Fig. 6A, the growth of both tumors was significantly suppressed compared with the control group, showing that treatment of a primary tumor with PDT + IT-DC confers suppression of the growth of untreated as well as treated tumors. To simulate the clinical scenario in which multiple tumors are present at sites distant from the primary tumor, mice were simultaneously inoculated s.c. in one flank (as above) and i.v. with CT26 tumor cells. This resulted in the seeding of both lungs and the growth of multiple pulmonary metastases. Although a few lesions were visible in the lungs of mice treated with PDT + IT-DC, as shown in Fig. 6B, PDT + IT-DC treatment of the s.c. tumor in such mice resulted in a significant reduction of the lung lesions compared with untreated control animals ($P < 0.05$). Representative examples of lungs from a healthy mouse, a tumor-bearing PDT + IT-DC–treated mouse, and an untreated (control) tumor-bearing mouse are shown in Fig. 6C, D, and E.

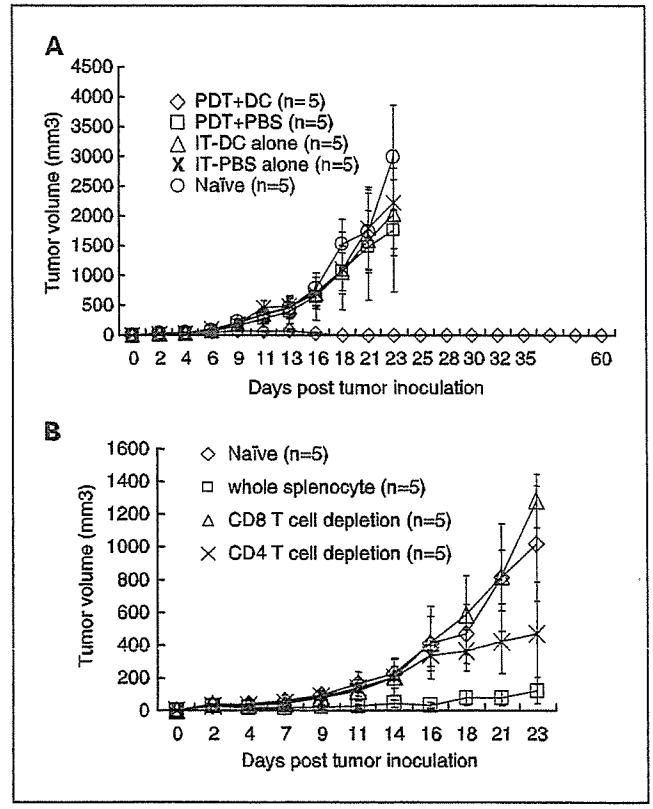

Fig. 5. *A*, adoptive transfer of splenocytes from PDT + IT-DC – treated mice to naïve mice prevents CT26 tumor growth. Splenocytes (1×10^7) from CT26 inoculated mice treated with IT-PBS alone (×), IT-DC alone (△), PDT + IT-PBS (□), or PDT + IT-DC (◇) were infused i.v. into naïve mice. One day later, the mice were challenged s.c. with a lethal number (1×10^6) of CT26 tumor cells. Naïve mice without splenocyte transfer were used as a control (○). Points, average tumor volume (mm^3) of five mice per group; bars, SE. *B*, role of CD4 and CD8 T-cell subsets in protection against CT26 tumors. Splenocytes were harvested from tumor-free mice treated with PDT + IT-DC. $CD4^+$ or $CD8^+$ T cells in splenocytes were depleted by using CD4 (L3T4) or CD8a (Ly-2) microbead magnetic cell sorting. After magnetic selection, whole splenocytes (□), CD4+ T-cell – depleted splenocytes (×), and CD8+ T-cell – depleted splenocytes (△) were infused i.v. into each of five naïve mice. Mice treated with splenocytes from naïve mice served as a control group (◇). One day later, these mice were s.c. challenged with a lethal number (1×10^6) of CT26 cells and monitored for tumor volume and survival.

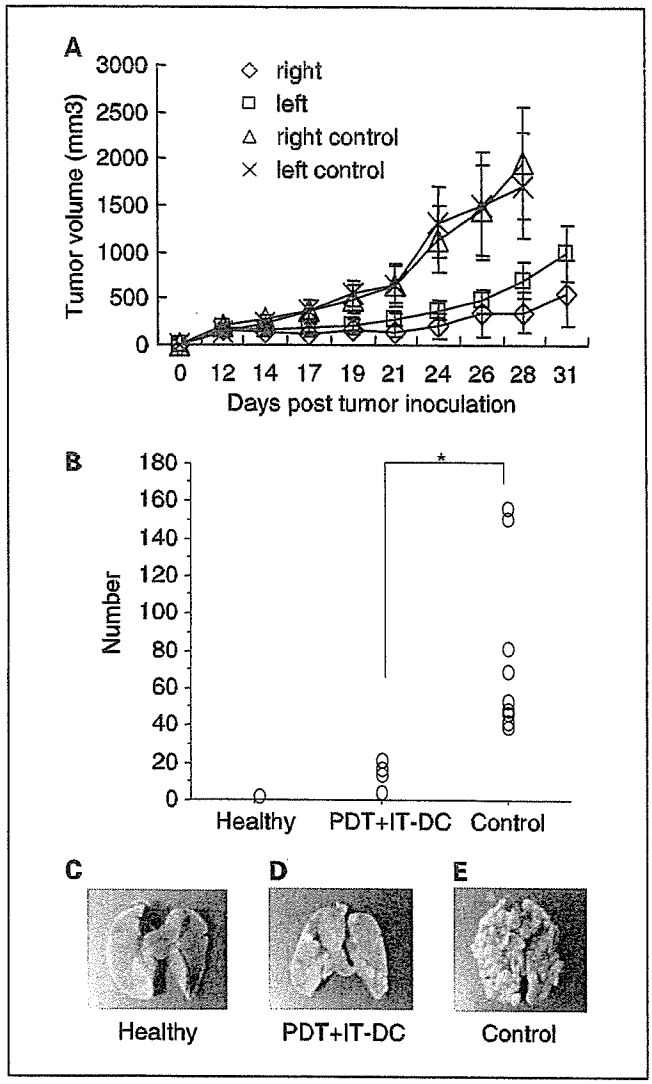

Fig. 6. Systemic tumor-specific immunity induced by local PDT + IT-DC treatment affects tumors at distant sites. *A*, CT26 tumor cells (1×10^6 for each side) were s.c. inoculated in both lower flanks of BALB/c mice. Twelve days later, the tumor-bearing mice were either untreated or treated with PDT + IT-DC into tumors on the right side but not the left side. Tumor growth on the left (untreated) and right (treated) sides was monitored and average tumor volume (±SE) was determined. Shown is the tumor volume on the right (with IT-PBS; △) and left (×) sides of control mice and the right (◇) and left (□) sides of treated mice. Each group contained five mice. *, $P < 0.05$, between left treated and control groups and between right treated and control groups. *B*, 10 BALB/c mice were inoculated s.c. with 1×10^6 CT26 tumor cells on day 0. On day 5, mice were injected i.v. with the same number of CT26 tumor cells, and on day 12, the s.c. tumors were treated with PDT + IT-DC. On day 26, lungs were harvested and stained with Bouin's solution to confirm and quantify lung metastases. *, $P < 0.05$, versus control group. *C*, representative lungs from a healthy mouse. *D*, representative lungs from a tumor-bearing PDT + IT-DC – treated mouse. *E*, representative lungs from an untreated control mouse.

Collectively, these data indicate that PDT + IT-DC therapy induces potent systemic tumor-specific immunity against CT26 colon cancer.

Discussion

One reason postulated for the limited clinical efficacy of most DC-based cancer vaccines studied to date is their variable ability to induce strong antitumor immunity, particularly CTL responses. This variability may have been due to problems related to tumor antigen selection or DC activation. Most DC-based clinical trials have included only a single or few tumor antigens although tumors contain thousands of potential antigens. Moreover, although a wide range of methods have been used to activate DCs and load them with antigens *in vitro*, there is no agreement about which of these methods induces optimal antitumor immunity. We sought to overcome these limitations by introducing unpulsed syngeneic DCs directly into tumors following treatment of the tumors with PDT, which creates a microenvironment that favors tumor antigen acquisition as well as activation of the DCs. The results confirm that PDT-treated tumors contain all of the factors necessary to activate DCs, load them with antigens, and induce an effective systemic antitumor immune response.

Although relatively little work has been done to evaluate the combination of PDT and IT-DC, several previous studies have shown the benefit of combining IT-DC with chemotherapy or radiotherapy (20–26). In contrast to chemotherapy or radiotherapy, PDT is not associated with systemic toxicity. Moreover, PDT renders murine tumors more immunogenic than tumors treated with UV or ionizing irradiation, or frozen and thawed tumors (27). Recently, Jalili et al. (28) reported that PDT in combination with IT-DC had little or no effect on s.c. CT26 tumors but inhibited the growth of contralateral tumors. By contrast, we observed dramatic effects on both local and distant tumors despite the fact that treatment was begun 12 days after inoculation of mice with a higher tumor dose than that studied by Jalili et al. One possible explanation for this surprising result is that we injected the same DC number four times as opposed to twice in their study. Another difference in our two studies is that Jalili et al. used the hematoprophyrin derivative, profimersodium (Photofrin), as a photosensitizer whereas we used ATX-S10 Na(II). Although Photofrin is widely used clinically, its potency is limited by weak absorbance at the shorter range of the red region of the spectrum. In addition, Photofrin is not a pure substance but a mixture of hematoporphyrin monomers, dimers, oligomers, and their dehydration products, and these products are associated with long-lasting skin photosensitivity (12). In contrast, ATX-S10 Na(II) is a homogeneous agent that preferentially accumulates in tumor tissues and is eliminated from normal tissues within 24 to 48 hours after injection. Moreover, its absorption maximum lies at 670 nm, which is longer than that of Photofrin (630 nm) and enables deeper tissue penetration (16). Using ATX-S10 Na(II) as a photosensitizer, we showed that PDT in combination with IT-DC inhibits the growth of two histologically distinct murine tumors. Interestingly, treatment of B16 tumors with combined PDT + IT-DC was at least as effective as it was for CT26, despite the poor immunogenicity of B16 and its well-documented resistance to PDT alone (29).

Our studies clearly show that PDT + IT-DC induces systemic antitumor immunity as well as tumor-specific immunologic memory. In the B16 model, the observation of white hair in untreated sites of mice, of which the tumors had been eradicated following PDT + IT-DC, suggests that treatment induced a systemic immune response against one or more shared antigens present in normal melanocytes as well as B16 tumors. In the CT26 model, PDT + IT-DC treatment of a single s.c. tumor resulted in regression of both contralateral as well as multiple

pulmonary tumors. The cells responsible for mediating tumor regression were cytotoxic T cells as indicated by both *in vitro* cytotoxicty assays and the observation that naïve animals were protected against tumors by adoptively transferred splenocytes from successfully treated tumor-bearing mice. Depletion of specific T-cell subsets (CD4 or CD8) in the adoptively transferred splenocytes indicated the CD8 T cells are the major effector cells induced by the PDT + IT-DC treatment.

Critical to the systemic antitumor effect of PDT + IT-DC is the capture of tumor-associated antigens by DCs as well as DC activation. Whether necrotic or apoptotic tumor cells serve as the superior source of tumor-associated antigens is controversial (30–34). Our data (not shown) strongly suggest that PDT, which induces both apoptosis and necrosis of tumors (12, 28), causes DCs to take up and process tumor antigen released by the dying tumor cells, mature, and become activated *in situ* and then cross-prime T cells against tumor-derived antigens. Interestingly, PDT alone had little or no effect on the growth of B16 tumors and analysis of such tumors following their treatment with PDT revealed a much smaller percentage of apoptotic and necrotic cells than in identically treated CT26 tumors (data not shown). Because PDT + IT-DC was effective as a treatment for both tumors, it seems likely that a relatively small number of dead or dying tumor cells can provide the necessary antigens required for DC-mediated induction of antitumor immunity. Furthermore, because it is known that PDT stimulates the expression of inflammatory cytokines such as tumor necrosis factor α, IL-1, and IL-6 (12, 13), perhaps the presence of such factors in the tumor microenvironment played a critical role in the induction of DC maturation.

In summary, the data presented in this report indicate that PDT + IT-DC results in potent systemic antitumor immunity and regression of tumors including tumors at sites distant from the treated site. Based on these findings, this novel regimen may prove beneficial in the treatment of patients with advanced metastatic disease as well as in the neoadjuvant setting before resection of tumors known to have a high recurrence rate.

Acknowledgments

We thank Claudia Benike, Linda Wu, and Ines Mende for critically reviewing the manuscript.

References

1. Hsu FJ, Benike C, Fagnoni F, et al. Vaccination of patients with B-cell lymphoma using autologous antigen pulsed dendritic cells. Nat Med 1996;2:52–8.
2. Steinman RM, Pope M. Exploiting dendritic cells to improve vaccine efficacy. J Clin Invest 2002;109: 1519–26.
3. Banchereau J, Palucka K. Dendritic cells as therapeutic vaccines against cancer. Nat Rev Immunol 2005;5: 296–306.
4. Fields RC, Shimizu K, Mule JJ. Murine dendritic cells pulsed with whole tumor lysates mediate potent antitumor immune responses *in vitro* and *in vivo*. Proc Natl Acad Sci U S A 1998;95:9482–7.
5. Song W, Kong HL, Carpenter H, et al. Dendritic cells genetically modified with an adenovirus vector encoding the cDNA for a model antigen induce protective and therapeutic antitumor immunity. J Exp Med 1997; 186:1247–56.
6. Boczkowski D, Nair SK, Snyder D, Gilboa E. Dendritic cells pulsed with RNA are potent antigen-presenting cells *in vitro* and *in vivo*. J Exp Med 1996;184:465–72.
7. Condon C, Watkins SC, Celluzzi CM, Thompson K, Falo LD, Jr. DNA-based immunization by *in vivo* transfection of dendritic cells. Nat Med 1996;2:1122–8.
8. Gong J, Chen D, Kashiwaba M, Kufe D. Induction of antitumor activity by immunization with fusions of dendritic and carcinoma cells. Nat Med 1997;3: 558–61.
9. Fong L, Engleman EG. Dendritic cells in cancer immunotherapy. Annu Rev Immunol 2000;18:245–73.
10. Engleman EG. Dendritic cell-based cancer immunotherapy. Semin Oncol 2003;30:23–9.
11. Figdor CG, De Vries JM, Lesterhuis WJ, Melief CJM. Dendritic cell immunotherapy: mapping the way. Nat Med 2004;10:475–80.
12. Dougherty TJ, Gomer CJ, Henderson BW, et al. Photodynamic therapy. J Natl Cancer Inst 1998;90: 889–905.
13. Gollnick SO, Liu X, Owczarczak B, Musser DA, Henderson BW. Altered expression of interleukin 6 and interleukin 10 as a result of photodynamic therapy *in vivo*. Cancer Res 1997;57:3904–9.
14. Engleman EG, Brody J, Soares L. Using signaling pathways to overcome immune tolerance to tumors. Sci STKE 2004; pe28.
15. Furumoto K, Soares L, Engleman EG, Merad M. Induction of potent antitumor immunity by *in situ* targeting of intratumoral DCs. J Clin Invest 2004; 113:774–83.
16. Mori M, Sakata I, Hirano T, et al. Photodynamic therapy for experimental tumors using ATX-S10(Na), a hydrophilic chlorin photosensitizer, and diode laser. Jpn J Cancer Res 2000;91:753–9.
17. Biel MA. Photodynamic therapy and the treatment of head and neck cancers. J Clin Laser Med Surg 1996;14:239–44.
18. Aruga A, Aruga E, Tanigawa K, Bishop DK, Sondak VK, Chang AE. Type 1 versus type 2 cytokine release by Vβ T cell subpopulations determines *in vivo* antitumor reactivity: IL-10 mediates a suppressive role. J Immunol 1997;159:664–73.
19. Barth RJ, Jr., Mule JJ, Spiess PJ, Rosenberg SA. Interferon γ and tumor necrosis factor have a role in tumor regressions mediated by murine CD8+ tumor-infiltrating lymphocytes. J Exp Med 1991;173: 647–58.
20. Tong Y, Song W, Crystal RG. Combined intratumoral injection of bone marrow-derived dendritic cells and systemic chemotherapy to treat pre-existing murine tumors. Cancer Res 2001;61:7530–5.
21. Tanaka F, Yamaguchi H, Ohta M, et al. Intratumoral injection of dendritic cells after treatment of anticancer drugs induces tumor-specific antitumor effect *in vivo*. Int J Cancer 2002;101:265–9.
22. Yu B, Kusmartsev S, Cheng F, et al. Effective combination of chemotherapy and dendritic cell administration for the treatment of advanced-stage experimental breast cancer. Clin Cancer Res 2003;9:285–94.
23. Shin JY, Lee SK, Kang CD, et al. Antitumor effect of intratumoral administration of dendritic cell combination with vincristine chemotherapy in a murine fibrosarcoma model. Histol Histopathol 2003;18:435–47.
24. Teitz-Tennenbaum S, Li Q, Rynkiewicz S, et al. Radiotherapy potentiates the therapeutic efficacy of intratumoral dendritic cell administration. Cancer Res 2003;63:8466–75.
25. Ehtesham M, Kabos P, Gutierrez MA, Samoto K, Black KL, Yu JS. Intratumoral dendritic cell vaccination elicits potent tumoricidal immunity against malignant glioma in rats. J Immunother 2003;26:107–16.
26. Song W, Levy R. Therapeutic vaccination against murine lymphoma by intratumoral injection of naive dendritic cells. Cancer Res 2005;65:5958–64.
27. Gollnick SO, Vaughan L, Henderson BW. Generation of effective antitumor vaccines using photodynamic therapy. Cancer Res 2002;62:1604–8.
28. Jalili A, Makowski M, Switaj T, et al. Effective photoimmunotherapy of murine colon carcinoma induced by the combination of photodynamic therapy and dendritic cells. Clin Cancer Res 2004;10:4498–508.
29. Schoenfeld N, Mamet R, Nordenberg Y, Shafran M, Babushkin T, Malik Z. Protoporphyrin biosynthesis in melanoma B16 cells stimulated by 5-aminolevulinic acid and chemical inducers: characterization of photodynamic inactivation. Int J Cancer 1994;56:106–12.
30. Albert ML, Sauter B, Bhardwaj N. Dendritic cells acquire antigen from apoptotic cells and induce class I-restricted CTLs. Nature 1998;392:86–9.
31. Steinman RM, Turley S, Mellman I, Inaba K. The induction of tolerance by dendritic cells that have captured apoptotic cells. J Exp Med 2000;191:411–6.
32. Sauter B, Albert ML, Francisco L, Larsson M, Somersan S, Bhardwaj N. Consequences of cell death: exposure to necrotic tumor cells, but not primary tissue cells or apoptotic cells, induces the maturation of immunostimulatory dendritic cells. J Exp Med 2000;191:423–34.
33. Gallucci S, Lolkema M, Matzinger P. Natural adjuvants: endogenous activators of dendritic cells. Nat Med 1999;5:1249–55.
34. Rovere P, Vallinoto C, Bondanza A, et al. Bystander apoptosis triggers dendritic cell maturation and antigen-presenting function. J Immunol 1998; 161:4467–71.

Immunohistochemical Differential Diagnosis Between Large Cell Neuroendocrine Carcinoma and Small Cell Carcinoma by Tissue Microarray Analysis With a Large Antibody Panel

Jun-ichi Nitadori, MD,[1,2,4] Genichiro Ishii, MD,[1] Koji Tsuta, MD,[1] Tomoyuki Yokose, MD,[1] Yukinori Murata, MT,[1] Tetsuro Kodama, MD,[3] Kanji Nagai, MD,[2] Harubumi Kato, MD,[4] and Atsushi Ochiai, MD[1]

Key Words: Lung cancer; Large cell neuroendocrine carcinoma; Small cell carcinoma; Tissue microarray; Immunohistochemistry; Large antibody panel

DOI: 10.1309/DT6BJ698LDX2NGGX

Abstract

To elucidate additional phenotypic differences between large cell neuroendocrine carcinoma (LCNEC) and small cell lung carcinoma (SCLC), we performed tissue microarray (TMA) analysis of surgically resected LCNEC and SCLC specimens. Immunostaining with 48 antibodies was scored based on staining intensity and the percentage of cells that stained positively. Four proteins were identified as significantly expressed in LCNEC as compared with SCLC: cytokeratin (CK)7, 113 vs 49 (P < .0301); CK18, 171 vs 60 (P < .0008); E-cadherin, 77 vs 9 (P < .0073); and β-catenin, 191 vs 120 (P < .0286). Immunostaining of cross-sections containing LCNEC and SCLC components revealed significant expression of CK7, CK18, and β-catenin in the LCNEC component compared with the SCLC component in 2 of 3 cases. Our results indicate that significant expression of CK7, CK18, E-cadherin, and β-catenin is more characteristic of LCNEC than of SCLC, and these findings provide further support that these tumor types are separate entities morphologically and immunophenotypically, if not biologically.

Lung cancer is a major cancer throughout the world and the most common cause of cancer mortality. The revised World Health Organization (WHO) classification of lung cancer published in 1999 classifies neuroendocrine tumors into 4 major histologic categories: low-grade malignant "typical" carcinoid, intermediate-grade malignant "atypical" carcinoid, and 2 high-grade tumors, large cell neuroendocrine carcinoma (LCNEC) and small cell lung carcinoma (SCLC).[1] In 1991, Travis et al[2] introduced the term *large cell neuroendocrine carcinoma* to describe a distinct category of high-grade neuroendocrine tumor with biologic and light microscopic characteristics different from those of high-grade SCLC. Morphologically, LCNEC is characterized by neuroendocrine morphologic features (rosette formation), large tumor cells (3 times larger in diameter than a small resting lymphocyte) with a low nuclear/cytoplasmic ratio, numerous nucleoli, a high mitotic rate (>10 in 10 high-power fields), a large degree of necrosis, and immunohistochemically staining positive for one or more neuroendocrine markers.

Some authors have reported that LCNEC has a poorer prognosis than SCLC,[3,4] whereas others have reported finding no significant difference in outcome between LCNEC and SCLC.[5-7] SCLC is sensitive to chemotherapy, but the optimal therapy for LCNEC has yet to be defined. Demetri et al[8] advocated that LCNEC be treated in a manner similar to SCLC but acknowledged that there may be a greater role for surgical resection in LCNEC. Nevertheless, it remains unclear how patients with LCNEC should be treated. Until now, few investigators have attempted to identify differences in molecular expression between LCNEC and SCLC. Sturm et al[9] reported a significantly higher frequency of thyroid transcription factor (TTF)-1 positivity with SCLCs, but no other biologic markers

with significantly different expression between LCNEC and SCLC have been reported.

Tissue microarray (TMA) analysis is becoming broadly accepted as an efficient and expeditious method in the field of proteomics,[10-12] and it provides a great deal of information that is equivalent to the information obtained from many tissue sections obtained from a large number of patients. It also is suitable for high-throughput molecular profiling of tumor specimens. In the present study, we used TMA with a large panel of antibodies to identify the phenotypic differences between LCNEC and SCLC.

Materials and Methods

Case Selection

During the period from January 1992 to December 2003, a total of 1,921 patients with primary lung carcinoma were treated at the National Cancer Center Hospital East, Chiba, Japan. All primary lung cancers with a pathologic diagnosis based on the classification schema of the third edition of the WHO classification[1] were reviewed, and 49 cases were diagnosed as LCNEC (2.6%). The 10 cases for which an adequate tissue specimen was not available for pathologic review were excluded from the study, leaving a total of 39 cases (2.0%) of LCNEC. TMA also was performed on specimens from 14 cases histologically diagnosed as pure SCLC (0.7%). In addition, 3 cases of SCLC combined with LCNEC were used to verify the results obtained by TMA.

Pathologic Studies

The specimens were fixed with 10% formalin and embedded in paraffin. Serial 4-μm sections were stained with H&E by the alcian blue–periodic acid–Schiff method for cytoplasmic mucin production and by the elastic van Gieson method for elastic fibers. Sections were reviewed by 3 pulmonary pathologists (J.N., G.I., and T.Y.) according to the histologic criteria described in the WHO classification criteria, and discrepancies were resolved by joint discussion of the slides viewed with a multiheaded microscope.

Construction of Tumor TMAs

The most representative tumor areas were selected carefully and marked on the H&E-stained slide for construction of microarrays. TMAs were assembled with a tissue-arraying instrument (Beecher Instruments, Silver Spring, MD).[10] The microarray system consists of thin-walled stainless steel needles approximately 2 mm in diameter and a stylet for transferring and removing the contents of the needle. The assembly is held in an x-y position guide that is manually adjusted with digital micrometers. Core samples are retrieved from selected regions of donor tissue and precisely arrayed in a new (recipient) paraffin block. Extra samples of the specimens were obtained routinely by collecting 2 replicate core samples of tumor in different areas. Specimens from the 39 cases of LCNEC **Image 1B** and **Image 1D** and 14 cases of SCLC **Image 1C** and **Image 1E** were punched, and core samples were mounted in the same donor blocks **Image 1A**.

Normal Control TMA

The normal control TMA was used as the positive control array for each staining. This slide was composed of esophagus, stomach, small intestine, large intestine, liver, pancreas, spleen, brain, heart, lung, skin, testis, kidney, prostate gland, breast, thyroid gland, and adrenal gland samples.

Antibodies and Immunohistochemical Staining

The 48 antibodies used in the study are listed in **Table 1**. Immunohistochemical staining was performed as follows: TMA donor blocks were cut into 4-μm sections and mounted on silane-coated slides. The sections were deparaffinized in xylene and dehydrated in a graded alcohol series, and endogenous peroxidase was blocked with 3% hydrogen peroxide in absolute methyl alcohol. Heat-induced epitope retrieval was performed for 20 minutes at 95°C with a 0.02-mol/L concentration of citrate buffer (pH 6.0). After the slides cooled at room temperature for 60 minutes, they were rinsed with deionized water and incubated overnight with primary antibodies. The slides then were washed 3 times with phosphate-buffered saline and incubated with the EnVision+ System-HRP (DAKO, Glostrup, Denmark). The reaction products were stained with diaminobenzidine and counterstained with hematoxylin. Some antibodies (Table 1) were used in an automated immunostainer (Ventana Medical Systems, Tucson, AZ) after antigen retrieval by microwave heating and citrate buffer.[13]

Identification of Positive Cases

The cases were evaluated in random order without knowledge of patient history. Each case in which more than 10% of the cancer cells reacted positively for an antibody were recorded as positive.

Calculation of Staining Scores

Immunostaining was scored based on the intensity of staining and the percentage of cells that stained positively. Whenever there was a disagreement, the slides were reviewed, and consensus was reached. Staining scores were calculated by multiplying the percentage of positive tumor cells per section (0% to 100%) by the immunohistochemical staining intensity. The sections were classified according to staining intensity as negative (total absence of staining), 1+ (weak staining), 2+ (moderate staining), or 3+ (strong staining), and the scores obtained ranged from 0 to 300. The staining scores obtained for 2 samples from the same specimen were calculated, and the result was recorded as the

DOI: 10.1309/DT6BJ698LDX2NGGX

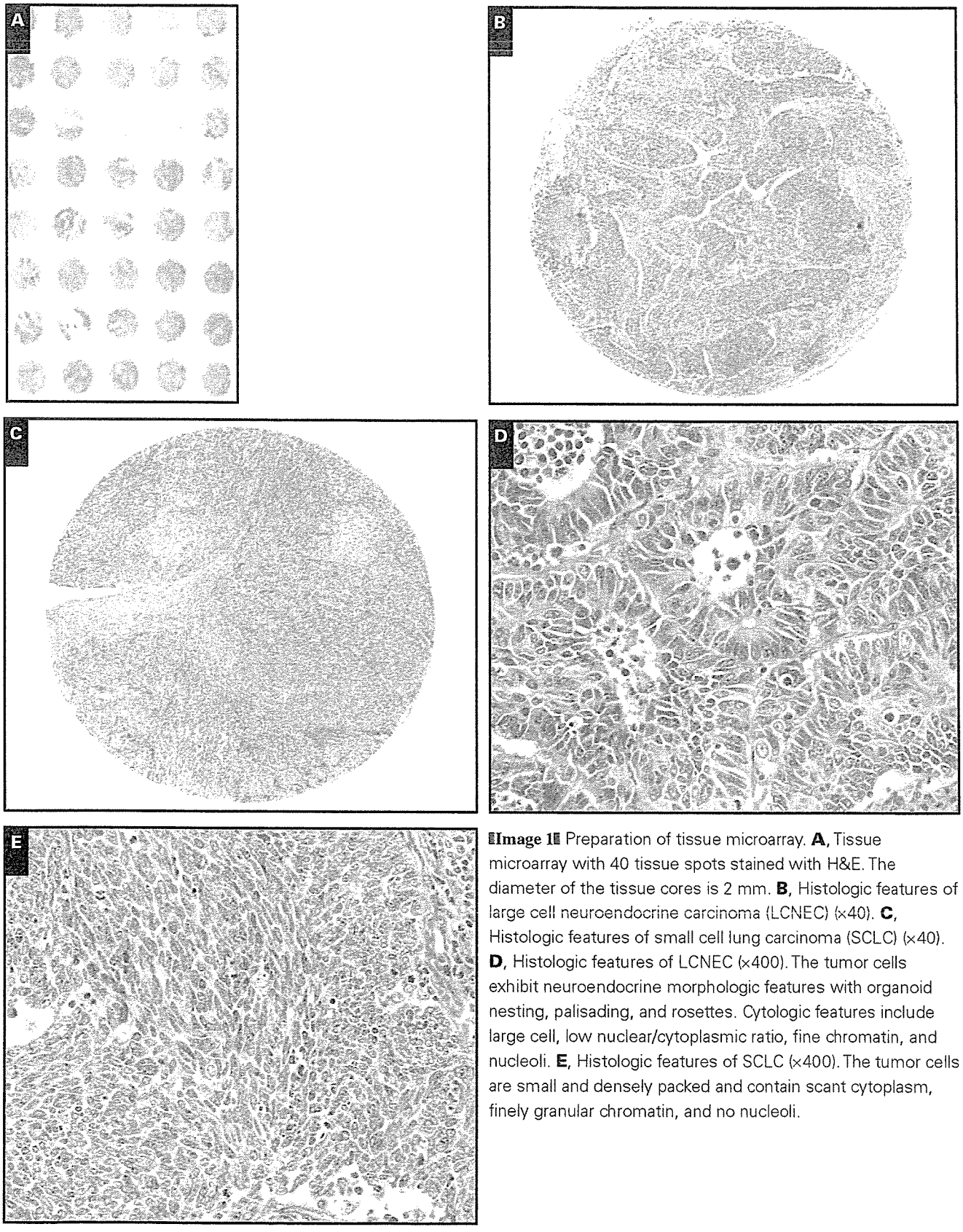

Image 1 Preparation of tissue microarray. **A**, Tissue microarray with 40 tissue spots stained with H&E. The diameter of the tissue cores is 2 mm. **B**, Histologic features of large cell neuroendocrine carcinoma (LCNEC) (×40). **C**, Histologic features of small cell lung carcinoma (SCLC) (×40). **D**, Histologic features of LCNEC (×400). The tumor cells exhibit neuroendocrine morphologic features with organoid nesting, palisading, and rosettes. Cytologic features include large cell, low nuclear/cytoplasmic ratio, fine chromatin, and nucleoli. **E**, Histologic features of SCLC (×400). The tumor cells are small and densely packed and contain scant cytoplasm, finely granular chromatin, and no nucleoli.

DOI: 10.1309/DT6BJ698LDX2NGGX